

## **Supplemental Text**

### *Gynecologists report:*

A 30-year old G1P0 was referred to our tertiary centre for targeted ultrasonography at 13 weeks due to abnormal profile. We noted an abnormal retronasal triangle, absence of the palate in sagittal view and a protruding median part of the maxilla, indicating a severe bilateral cheilognathopalatoschisis. Forearms and hands were structurally normal but afunctional. Both feet were abnormally positioned. Termination of pregnancy on the couple's request was performed at 14 weeks. Consent was given to publish photographs and molecular data.

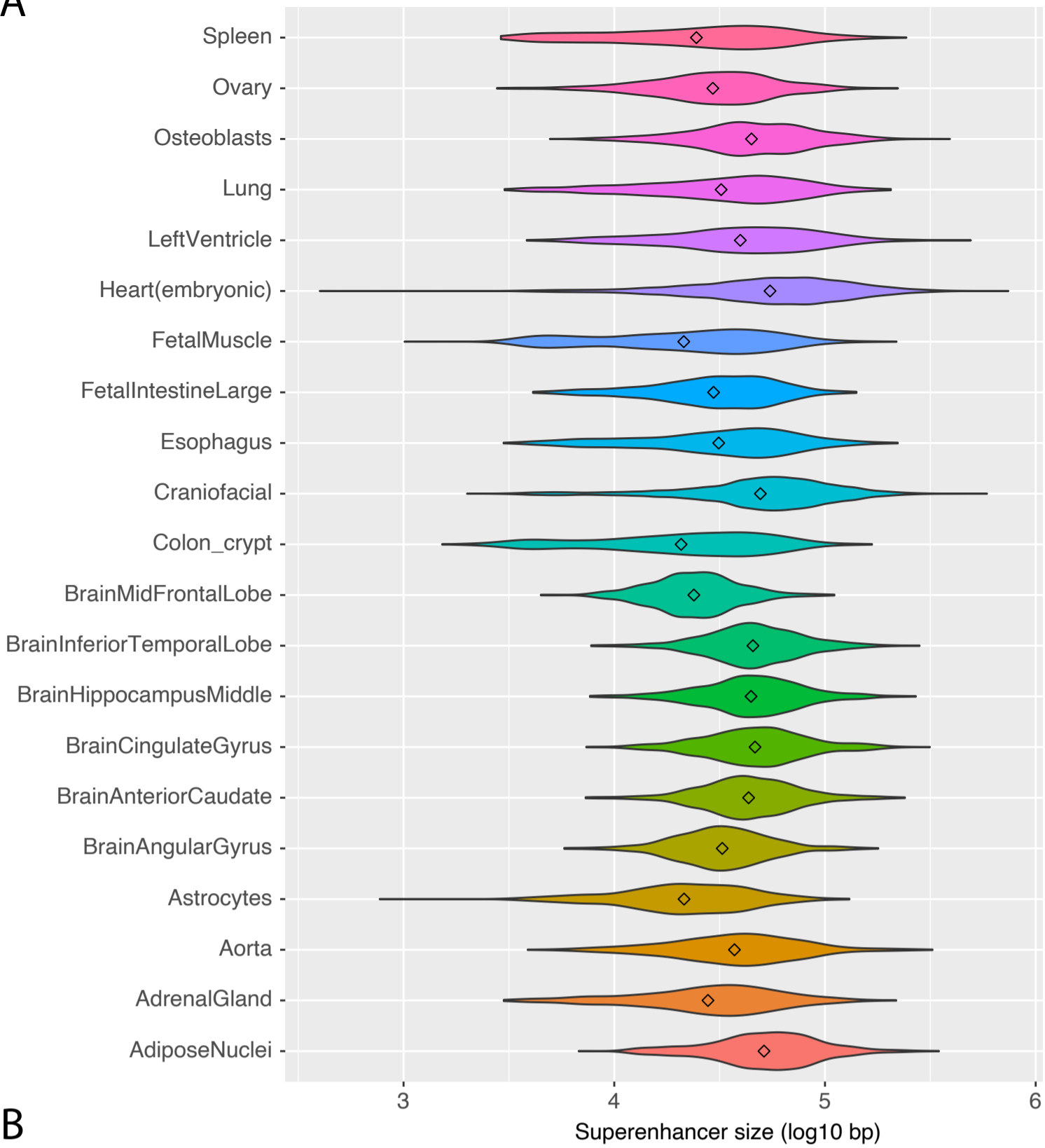
For the second case report consent was given to publish Magnetic Resonance Imaging (MRI), Computed Tomography (CT) Images, and molecular data.

16 Supplemental Tables and 29 Supplemental Figures



**Figure S1-** Jaccard similarity of superenhancer sequences in human embryonic craniofacial tissue samples.

A



B

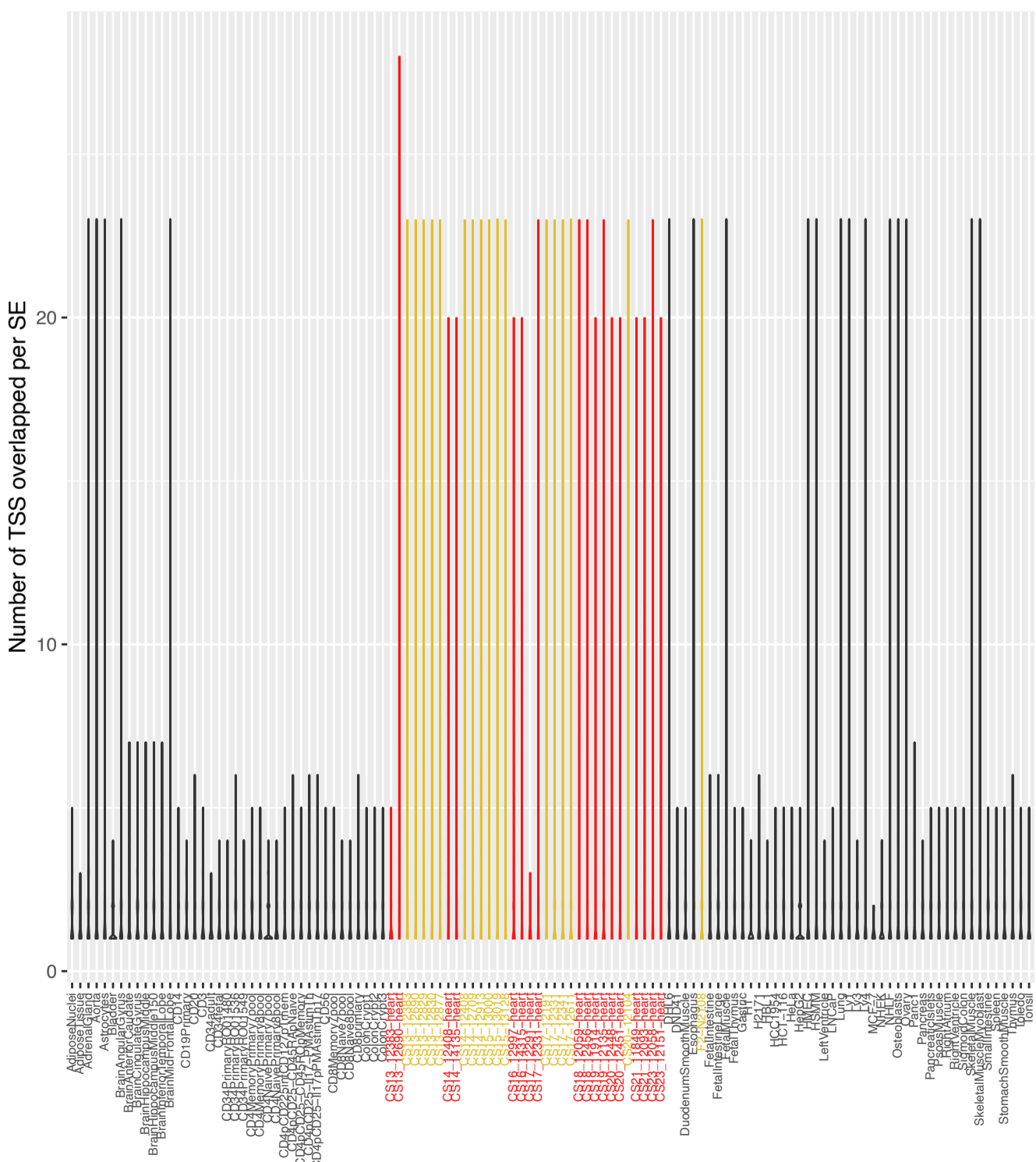


**Figure S2-** Violin plots of number of transcription start sites (TSSs) overlapped by superenhancers in various tissues. Plots in black reference tissues and cell types in the dbSuper database. Plots in yellow are the results from human embryonic craniofacial tissue. Plots in red are the results from human embryonic heart. Superenhancers encompassing at minimum 1 and as many as 23 TSSs are found across multiple tissues. Median number of TSSs for protein-coding genes encompassed by superenhancers in dbSuper tissues and cell lines = 1. Median number of TSSs for protein coding genes encompassed by superenhancers in craniofacial and heart samples ranged from 1-3.

# DisGeNET Disease Ontology Terms from Genes Nearest Non-overlapping CF-specific SEs

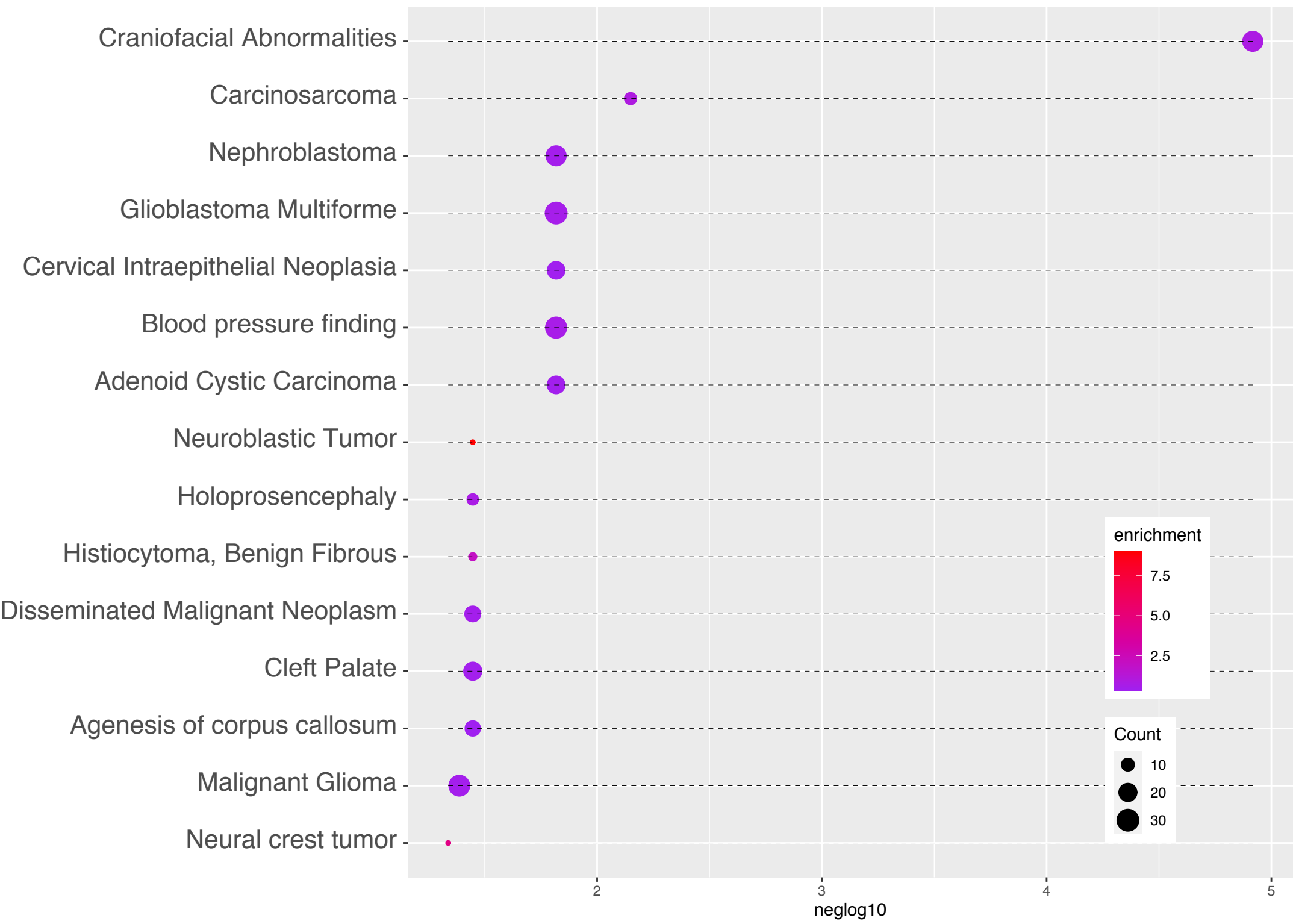


**Figure S3-** Biological Process Gene Ontology terms enriched in genes assigned to superenhancers in non-coding regions. Assignment of the two nearest genes was done through the BedTools suite function “closest”.

# Biological Process Gene Ontology Terms from Genes Nearest Non-overlapping CF-specific SEs

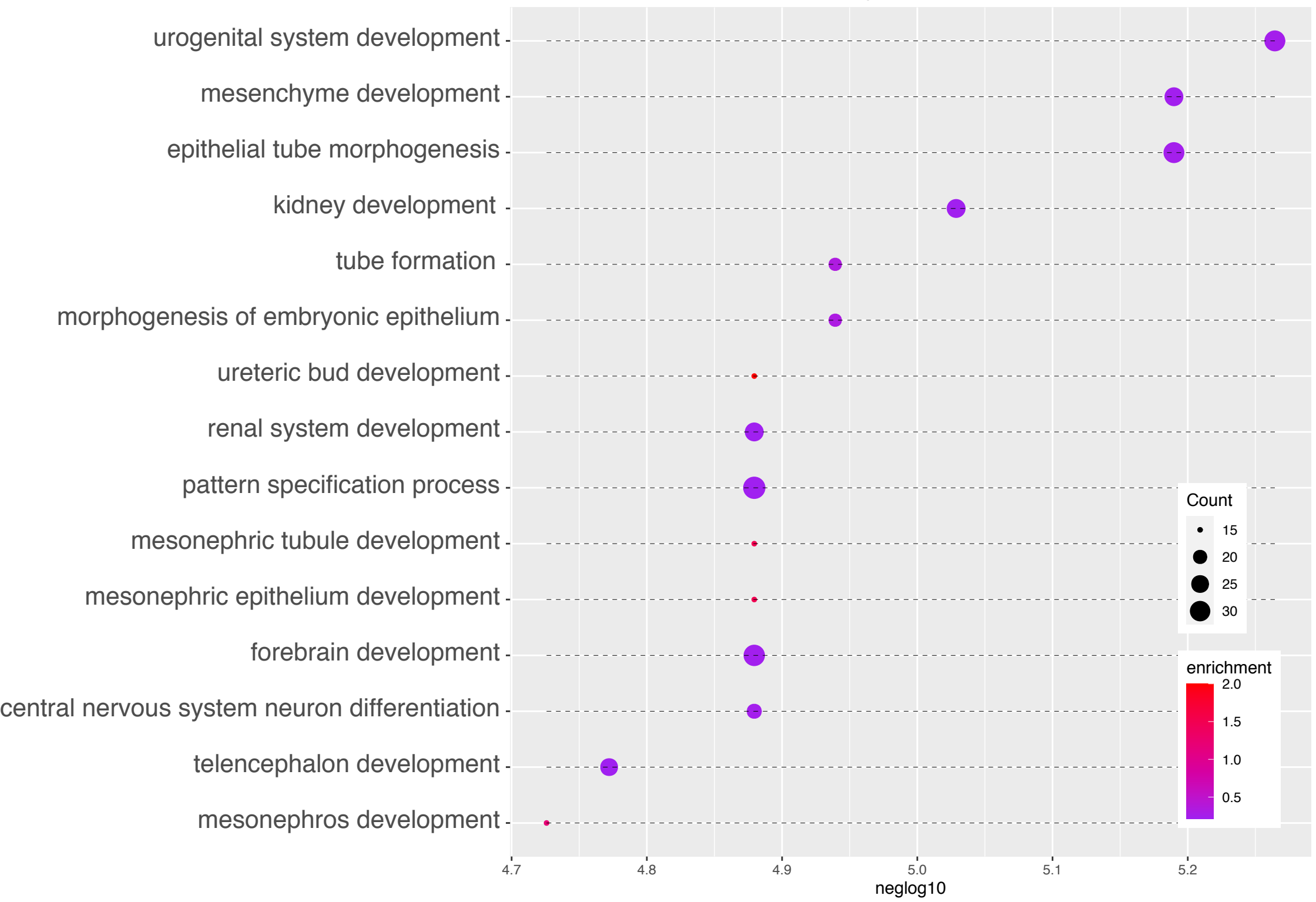




**Figure S4-** Disease Ontology terms from DisGeNet enriched in genes assigned to superenhancers in non-coding regions. Assignment of the two nearest genes was done through the BEDTools suite function “closest”.

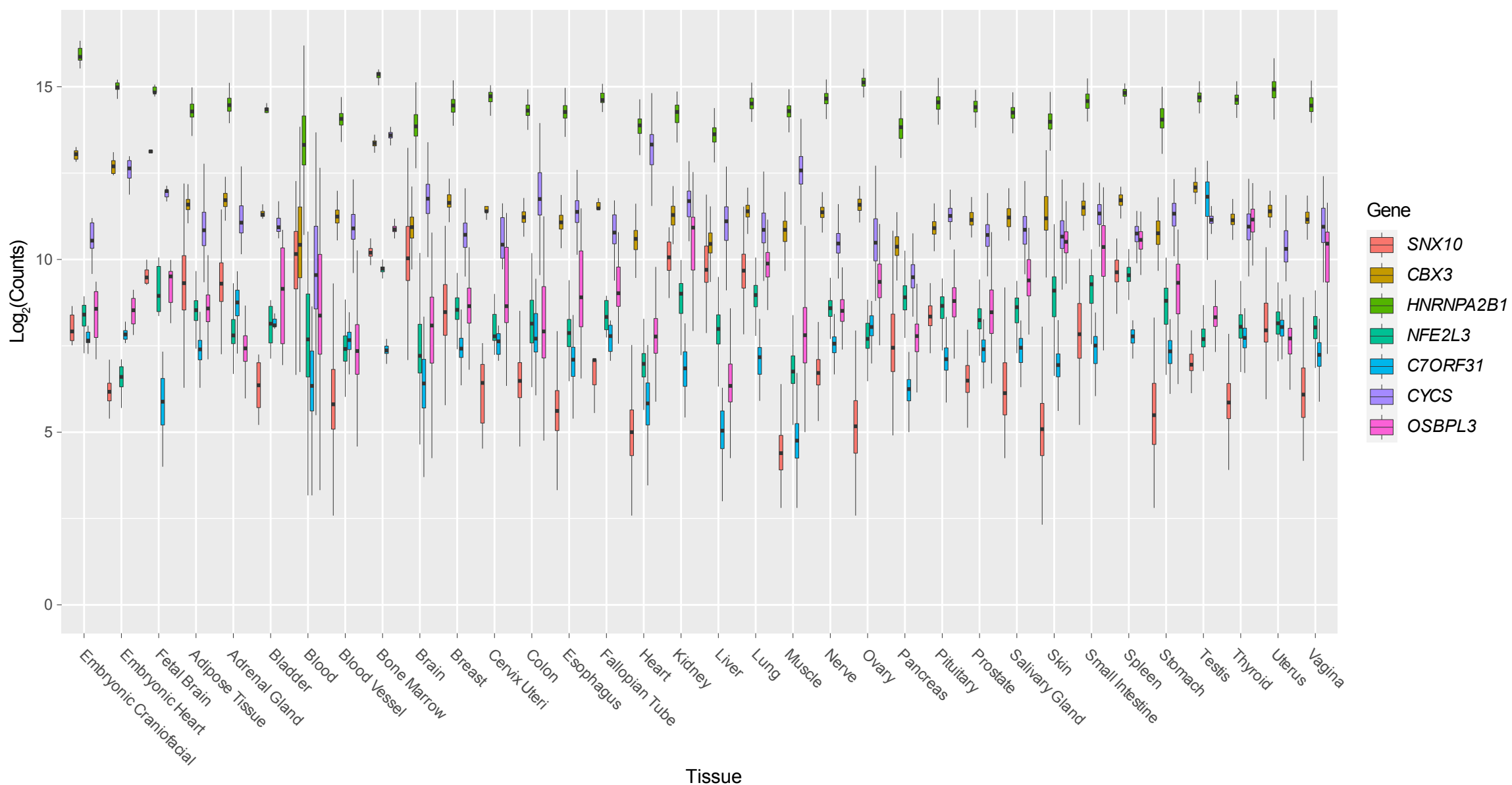


**Figure S5- Expression of genes within 500kb of gene desert.**

The  $\log_2 + 1$  of counts from human primary craniofacial tissue, embryonic heart, fetal brain and 31 adult tissues from GTEx. These genes show ubiquitous expression across all tissues surveyed.

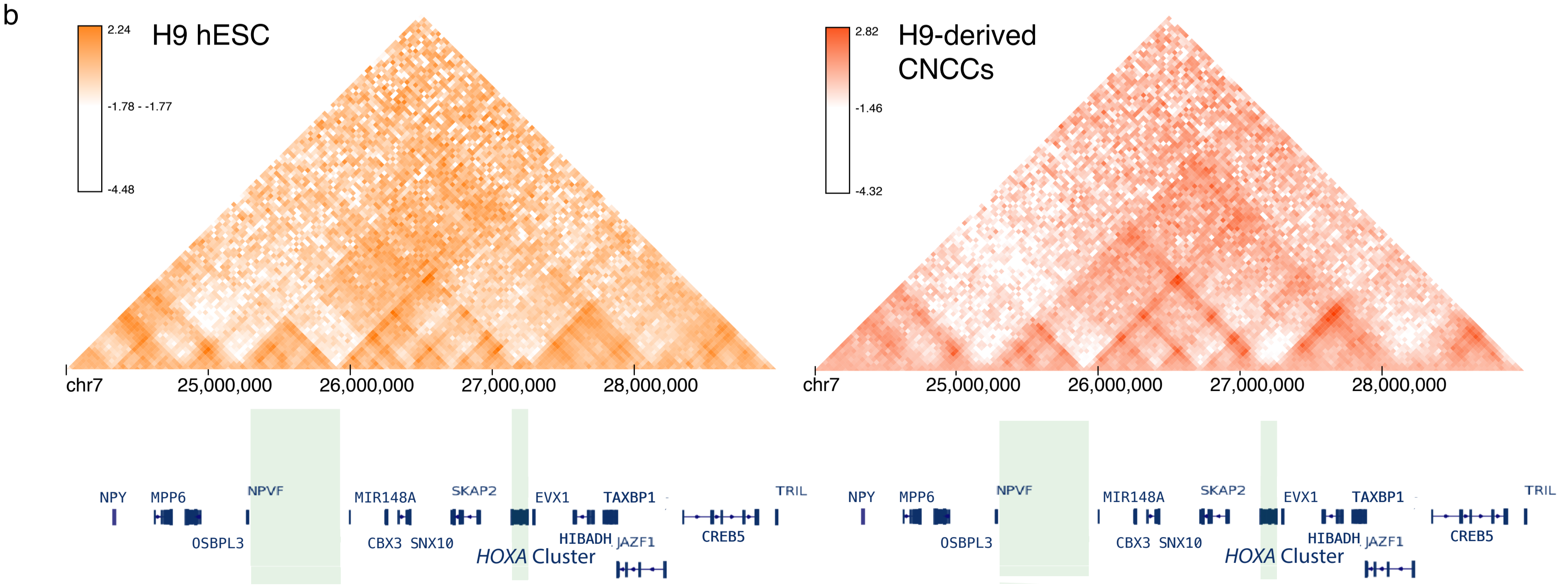
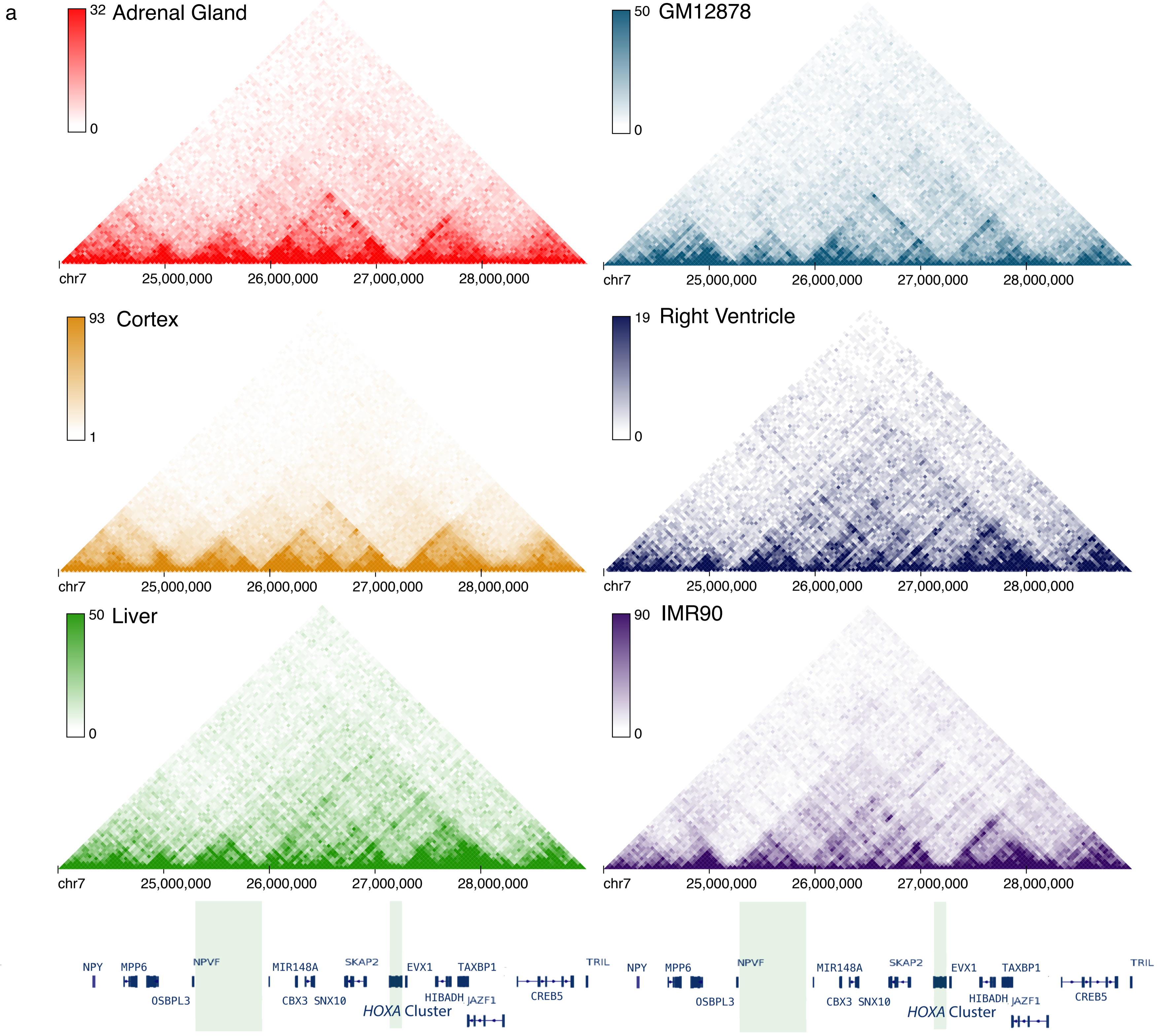


**Figure S6-** HiC from publicly available data of various human tissues and cell lines (a) and publicly available data from H9 (b- left) and H9-derived CNCCs (this study, b-right). Plots were generated through the HiC Browser hosted by Northwestern University. *HOXA* cluster and putative novel superenhancer region are highlighted with green shading.

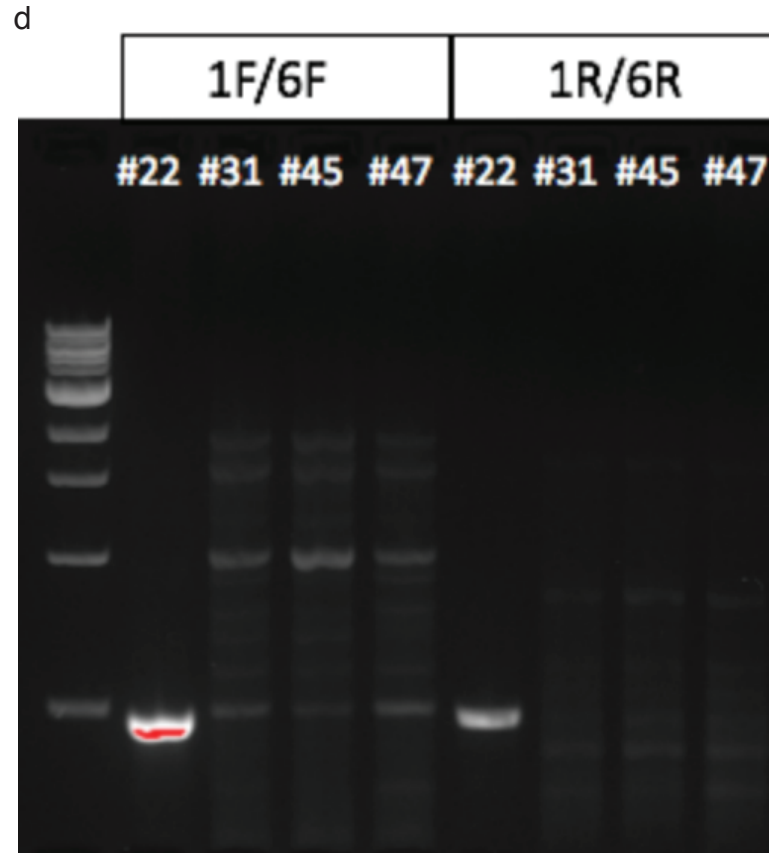
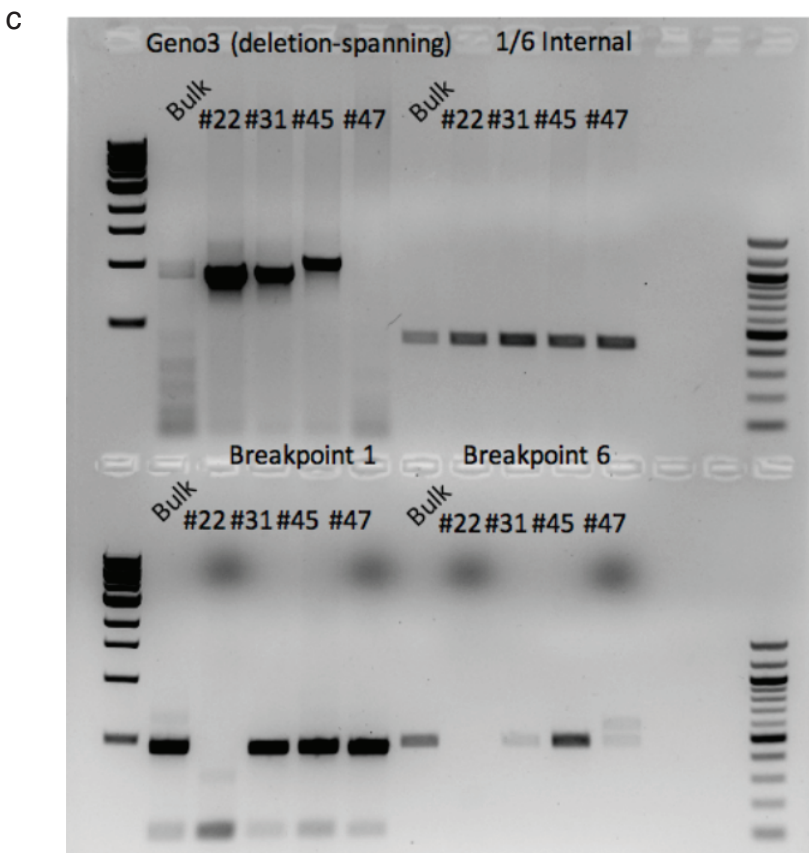
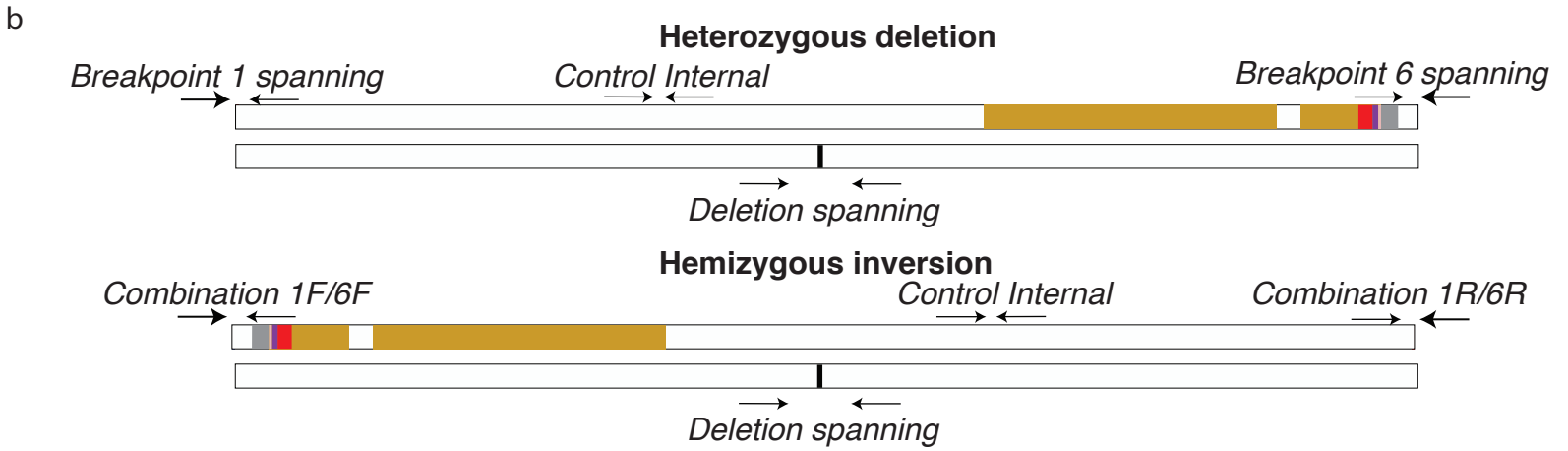
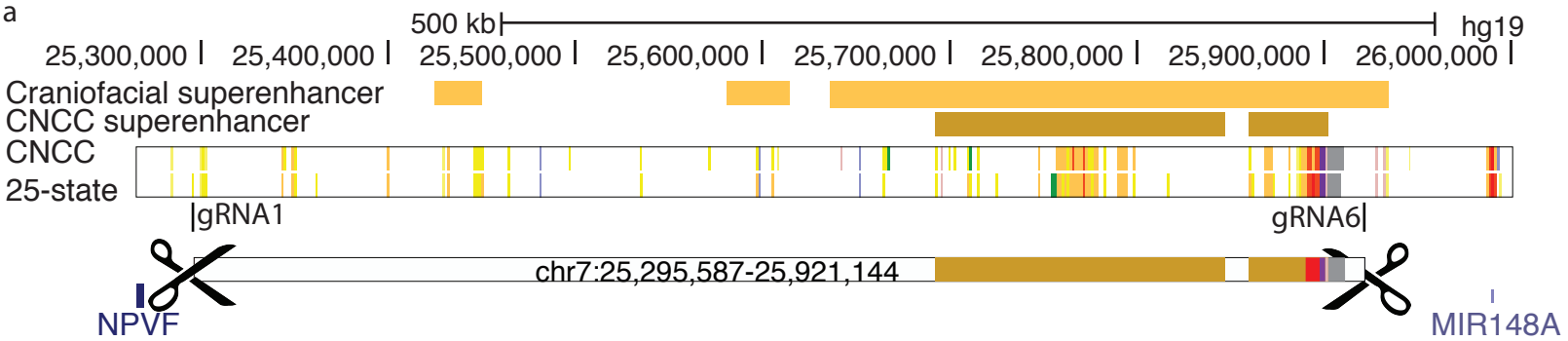


**Figure S7-** a. Location of guide RNAs gRNA1 and gRNA6 relative to the WT orientation. b. Screening strategy for determining whether clones are heterozygous for the 1/6 deletion and determining if a clone contains an inversion of the targeted region. c-d. PCR results identifying heterozygous clones and the clone carrying the hemizygous inversion (#22, also referred to as INV).







Clone\_31\_Geno3F GGTGGGGCGGGTAGCACAATTCAAATGTGACATTCTACAGTTCAGCTCAAAAAGAAGCAAT  
|||||  
Clone\_31\_Geno3R GGTGGGGCGGGTAGCACAATTCAAATGTGACATTCTACAGTTCAGCTCAAAAAGAAGCAAT

Clone\_31\_Geno3F TGGCTGATTGTCACCAAGTGACCTCACTTTGCTCTGCAGTTATCAGCATGGGAAGATATA  
|||||  
Clone\_31\_Geno3R TGGCTGATTGTCACCAAGTGACCTCACTTTGCTCTGCAGTTATCAGCATGGGAAGATATA

Clone\_31\_Geno3F AAACAGGTGAACCTGTGAATGTACACTGGTTTTAAACAGAGATAGAGGATGTAAAAGTCA  
|||||  
Clone\_31\_Geno3R AAACAGGTGAACCTGTGAATGTACACTGGTTTTAAACAGAGATAGAGGATGTAAAAGTCA

Clone\_31\_Geno3F TTCTGAAGCATATGGGAGGAGCTGCTTCTACAAACCTGATTTCCAGCTGCACAGTGGGA  
|||||  
Clone\_31\_Geno3R TTCTGAAGCATATGGGAGGAGCTGCTTCTACAAACCTGATTTCCAGCTGCACAGTGGGA

Clone\_31\_Del\_spanning\_F TCAGAGGAGCAGGGCCGGGCTATCATAAATCCCAGCAGGGGTGGGAGAACGTAAG  
|||||  
Clone\_31\_Del\_spanning\_R TCAGAGGAGCAGGGCCGGGSACTGGATCATAAATCCCAGCAGGGGTGGGAGAACGTAAG

Clone\_31\_Geno3F ACAGATTGCTAACACCTTaaaaaaaaaagtttaataaaaaaGGCAGGAATTTTCTTTAA  
|||||  
Clone\_31\_Geno3R ACAGATTGCTAACACCTTAAAAAAAAAAGTTTAAATAAAAAAGGCAGGAATTTTCTTTAA

Clone\_31\_Geno3F AGTATACCAAGCCCAGCAGGGACTGGGAGATACACAAGGCGGCTGAAGGAGGGAGCTACT  
|||||  
Clone\_31\_Geno3R AGTATACCAAGCCCAGCAGGGACTGGGAGATACACAAGGCGGCTGAAGGAGGGAGCTACT

Clone\_31\_Geno3F TTACCTTCCCAAGATCACTTTTCCGAGAAGCCCAAACCACAGAAAACCATTTCTGGCAGGT  
|||||  
Clone\_31\_Geno3R TTACCTTCCCAAGATCACTTTTCCGAGAAGCCCAAANCACAGAAAACCATTTCTGGCAGGT

Clone\_31\_Geno3F AAATCGGGCCCCATGAGCTTTTCATCAAAGCCAAGGATGTCTCTCTGGGATGTGTGTTA  
|||||  
Clone\_31\_Geno3R AAATCGGGCCCCANNNNNNTTTCATCAAAGCCAAGGATGTCTCTCTGGGATGTGTGTTA

Clone\_31\_Geno3F GAGATAAGGCAG  
|||||  
Clone\_31\_Geno3R GAGATAAGGCAG



Clone 22 at inversion

```

Clone_22_1F      nnnnnnnnnn nnnnnnnnnn nnnntggnnn nnnntnnnnc agngnngnnt 50
+Reference_hg19      25295459      T

Clone_22_1F      gtgaatgtac actgggtttta aacagagata gnnnnnnnaa aagtcattct 100
+Reference_hg19  GTGAATGTAC ACTGGTTTTA AACAGAGATA GaggatgtAA AAGTCATTCT

Clone_22_1F      gaagcatatg ggaggagctg cttnnncaaa cctgatttcc cagctgcaca 150
+Reference_hg19  GAAGCATATG GGAGGAGCTG CTTctaCAAA CCTGATTTC CAGCTGCACA

Clone_22_1F      gtgggatcag aggagcaggg ccggggaCGT ATTTTACTAC ACGATCTTGG
+Reference_hg19  GTGGGATCAG AGGAGCAGGG CCGGGGAC 25295587
-Reference_hg19      25921143  GT ATTTTACTAC ACGATCTTGG

Clone_22_1F      CAGGCTCCCC TCGTTGAAAT TCAAACCGAA GCAACTCaAT GGGGGAACAG 250
-Reference_hg19  CAGGCTCCCC TCGTTGAAAT TCAAACCGAA GCAACTCgAT GGGGGAACAG

Clone_22_1F      ACATAAAAAT ATTAATTTGG TAGATATTAA AAAAAATCAC ACTGGTTATA 300
-Reference_hg19  ACATAAAAAT ATTAATTTGG TAGATATTAA AAAAAATCAC ACTGGTTATA

Clone_22_1F      AATCAGGGGC TGTCCACTGG TTCCTTTCAT CATCTAAATG GTCCTTCTAA 350
-Reference_hg19  AATCAGGGGC TGTCCACTGG TTCCTTTCAT CATCTAAATG GTCCTTCTAA

Clone_22_1F      CCAGACTACA AATCTTACTG GAAAGCAGGA GGGGGTTTGG AAGGTGGGGG 400
-Reference_hg19  CCAGACTACA AATCTTACTG GAAAGCAGGA GGGGGTTTGG AAGGTGGGGG

Clone_22_1F      TCCCCTTCTT GAGGCTTTGG AGACAGCTTA CATCCAACAC TTCCTCAAAC 450
-Reference_hg19  TCCCCTTCTT GAGGCTTTGG AGACAGCTTA CATCCAACAC TTCCTCAAAC

Clone_22_1F      CTGGCTTTGa
-Reference_hg19  CTGGCTTTG 25920862

Clone_22_6F      nnnnnnnnnn nntgnnnnnn nnnnnnnnga nngganccc caaccttnna 50
      agccccctcct gctttccagt aagatttgta gnnnnnnnan aaggaccatt 100
+Ref_hg1925920937  CCCCTCCT GCTTTCAGT AAGATTTGTA GtctggttAg AAGGACCATT

Clone_22_6F      tagatgatga aaggaaccag tggacagccc ctgatttata accagtgtga 150
+Ref_hg19      TAGATGATGA AAGGAACCAG TGGACAGCCC CTGATTTATA ACCAGTGTGA

Clone_22_6F      ttttttttaa tatctaccaa attaatatTT ttatgtctgt tccccatttg 200
+Ref_hg19      TTTTTTTTAA TATCTACCAA ATTAATATTT TTATGTCTGT TCCCCATcG

Clone_22_6F      agttgcttcg gtttgaattt caacgagggg agcctgcca gaCGTGTAG 250
+Ref_hg19      AGTTGCTTCG GTTTGAATTT CAACGAGGGG AGCCTGCCAA GATCGTGTAG

Clone_22_6F      TAAAATACGT CCCC GGCCCT GCTCCTCTGA TCCCACTGTG CAGCTGGGAA 300
+Ref_hg19      TAAAATAC 25921143
-Ref_hg19 25295587  GT CCCC GGCCCT GCTCCTCTGA TCCCACTGTG CAGCTGGGAA

Clone_22_6F      ATCAGGTTTG TAGAAGCAGC TCCTCCATA TGCTTCAGAA TGACTTTTAC 350
-Ref_hg19      ATCAGGTTTG TAGAAGCAGC TCCTCCATA TGCTTCAGAA TGACTTTTAC

Clone_22_6F      ATCCTCTATC TCTGTTTAAA ACCAGTGAC ATTCACAGGT TCACCTGTTT 400

```

```

-Ref_hg19      ATCCTCTATC TCTGTTTAAA ACCAGTGTAC ATTCACAGGT TCACCTGTTT

Clone_22_6F   TATATCTTCC CATGCTGATA ACTGCAGAGC AAAGTGAGGT CACTTGGTGA 450
-Ref_hg19     TATATCTTCC CATGCTGATA ACTGCAGAGC AAAGTGAGGT CACTTGGTGA

Clone_22_6F   CAATCAGCCA A
-Ref_hg19     CAATCAGCCA A 25295385

Clone_22_1R   nnnnnnnnnn nnnnnnnnnn nntgnnnnnt aaatatgatg cacagnanca 50
-Ref_hg19     25295806                T AAATATGATG CACAGtAaCA

Clone_22_1R   ntggcggtgt gtaactagta gcgaatttgn nnnnnnnnnn gagaacattt 100
-Ref_hg19     gTGGCGGTGT GTAAC TAGTA GCGAATTTGa aaaccaaactctGAGAACATTT

Clone_22_1R   ggtggcttga ttaatttgc tgcgcnatcc gccatctggt gttgtctcca 150
-Ref_hg19     GGTGGCTTGA TTAATTTGCT TtGCCcATCC GCCATCTGTT GTTGTCTCCA

Clone_22_1R   ggagcccagg atggggcacc ctgcttgatt ctgctgactt aggccacctg 200
-Ref_hg19     GGAGCCCAGG ATGGGGCACC CTGCTTGATT CTGCTGACTT AGGCCACCTG

Clone_22_1R   gaagctctcc ttctataggg agtgggggtg gactctgctg aacaaaagt 250
-Ref_hg19     GAAGCTCT CTTCTATAG GGAGTGGGGGTG GACTCTGCTG AACAAAAGT 25295586
+Ref_hg19                                25921144

Clone_22_1R   ACTGGATCAT AAATCCCAGC AGGGGTGGGA GAACGTAAGA CAGATTGCTA 300
+Ref_hg19     ACTGGATCA TAAATCCCAG CAGGGGTGGG AGAACGTAAG ACAGATTGCTA

Clone_22_1R   ACACCTTAAA AAAAAAAGTT TAAATAAAAA AGGCAGGAAT TTTCTTTAAA 350
+Ref_hg19     ACACCTTAA AAAAAAAGT TAAATAAAAA AAGGCAGGAA TTTTCTTTAAA

Clone_22_1R   GTATACCAAG CCCAGCAGGG ACTGGGAGAT ACACAAGGCG GCTGAAGGAG 400
+Ref_hg19     GTATACCAA GCCCAGCAGG GACTGGGAGA TACACAAGGC GGCTGAAGGAG

Clone_22_1R   GGAGCTACTT TACCTTCCCA AGATCACTTT TCCGAGtAGC CCAAACCACA 450
+Ref_hg19     GGAGCTACT TTACCTTCCC AAGATCACTT TTCCGAGaAG CCAAACCACA

Clone_22_1R   GAAAACCATT CTGGCAa
+Ref_hg19     GAAAACCAT TCTGGCA 25921360

Clone_22_6R   nnnnnnnnnn nnnnnnnnnn nnntgngnnn gnnagtanct cctccttca 50
-Ref_h19                                25921303 AGTAGtCT CCCTCCTTCA

Clone_22_6R   gccgccttgt gtatctccca gtccttgcctg gnnttggtat actttaaaga 100
-Ref_h19     GCCGCCTTGT GTATCTCCCA GTCCTTGCCTG GgcTTGGTAT ACTTTAAAGA

Clone_22_6R   aaattcctgc cttttttatt taaacttttt tttttaaggt gtttagcaatc 150
-Ref_h19     AAATTCCTGC CTTTTTTATT TAAACTTTTT TTTTAAAGGT GTTAGCAATC

Clone_22_6R   tgtcttaagt tctcccaccc ctgctgggat ttatgatcca gttACTTTTG 200
-Ref_h19     TGTCTTACGT TCTCCCACCC CTGCTGGGAT TTATGATCCA GT 25921144
+Ref_h19                                25295586                ACTTTTG

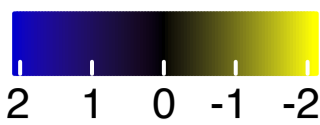
Clone_22_6R   TTCCGCAGAG TCCACCCCA CTCCTATAG AAGGAGAGCT TCCAGGTGGC 250
+Ref_h19     TTCCGCAGAG TCCACCCCA CTCCTATAG AAGGAGAGCT TCCAGGTGGC

```

Clone_22_6R	CTAAGTCAGC	AGAATCAAGC	AGGGTGCCCC	ATCCTGGGCT	CCTGGAGACA	300
+Ref_h19	CTAAGTCAGC	AGAATCAAGC	AGGGTGCCCC	ATCCTGGGCT	CCTGGAGACA	
Clone_22_6R	ACAACAGATG	GCGGATGGGC	AAAGCAAATT	AATCAAGCCA	CCAAATGTTC	350
+Ref_h19	ACAACAGATG	GCGGATGGGC	AAAGCAAATT	AATCAAGCCA	CCAAATGTTC	
Clone_22_6R	TCAGATTTGG	TTTTCAAATT	CGCTACTAGT	TACACACCGC	CACTGTTACT	400
+Ref_h19	TCAGATTTGG	TTTTCAAATT	CGCTACTAGT	TACACACCGC	CACTGTTACT	
Clone_22_6R	GTGCATCATA	TTTACTTGAC	AGCATTGTCC	AGTCCTTAGA	TTTCTCTCAC	450
+Ref_h19	GTGCATCATA	TTTACTTGAC	AGCATTGTCC	AGTCCTTAGA	TTTCTCTCAC	
Clone_22_6R	TGGCTCACGC	TAAAGAAa				
+Ref_h19	TGGCTCACGC	TAAAGAA	25295859			

**Figure S8-** (Word document) Sequence across breakpoints for clones #31 (heterozygous) and #22 (inversion, INV). Clone sequence based on Sanger sequencing results (see Methods) and compared against hg19 assembly.

# Z-score



WT

INV

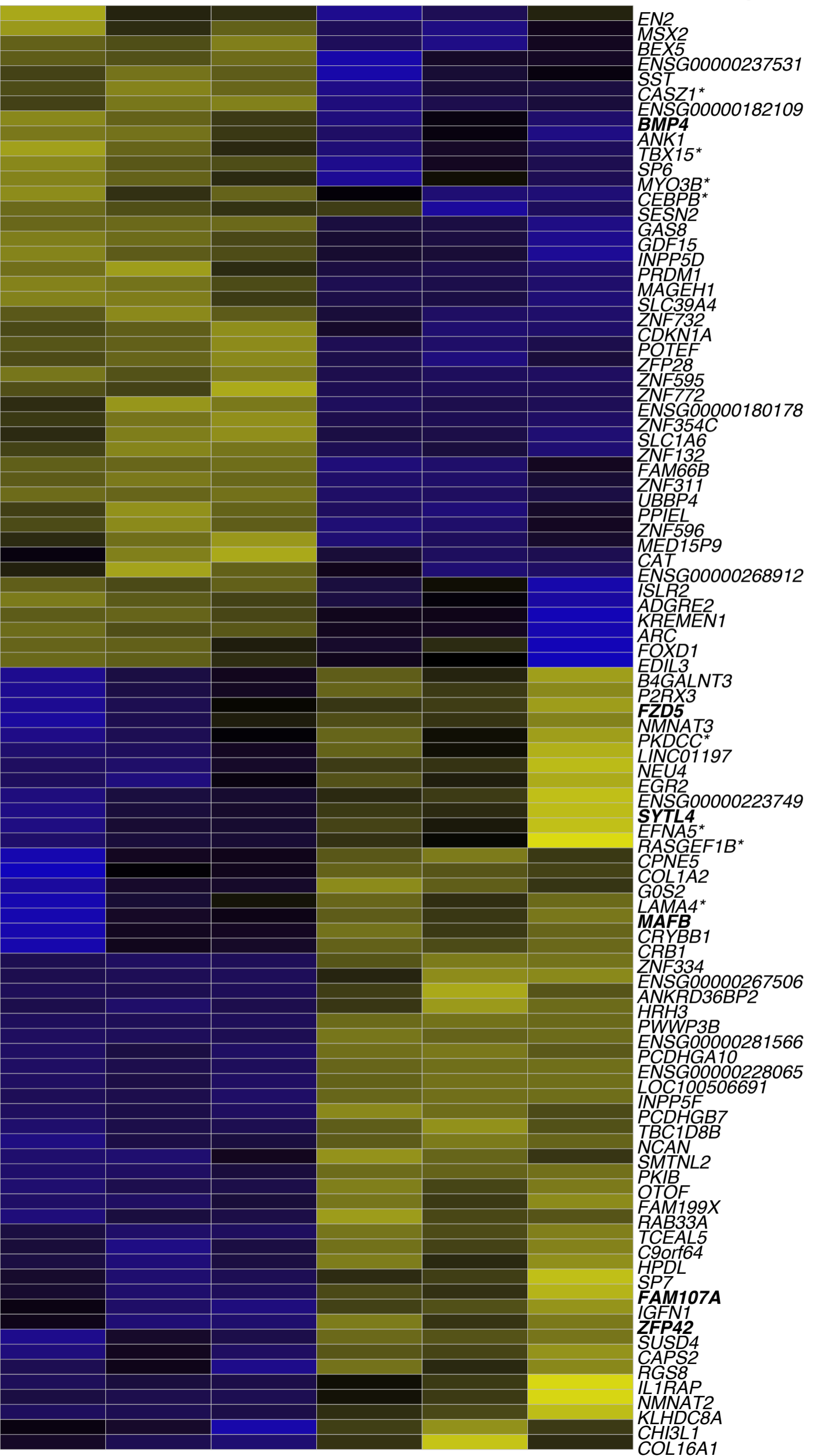
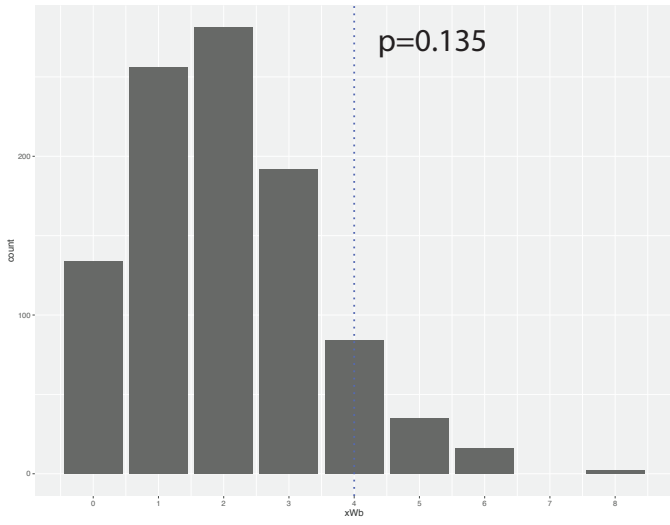


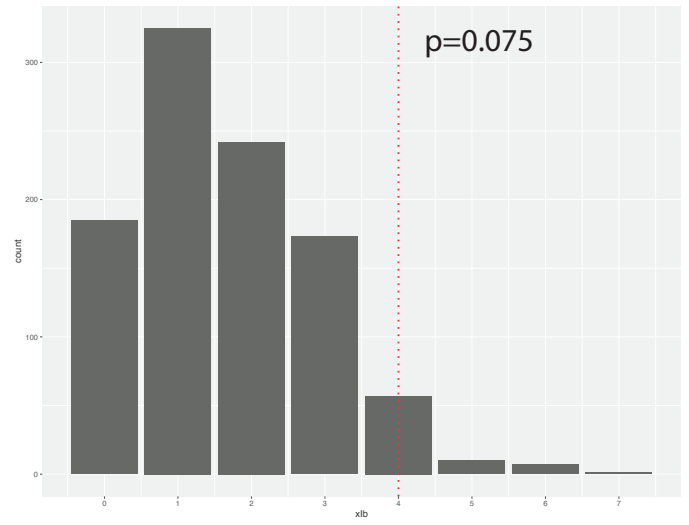


**Figure S9-** Heatmap of differentially expressed genes between WT and INV CNCCs. Names followed by asterisks are HOXA2 targets as determined by HOXA2 ChIP-seq (Donaldson et al. 2012). Names in bold are HOXA2 associated genes as determined by RNA-seq from *Hoxa2*<sup>-/-</sup> mice (Donaldson et al., 2012).

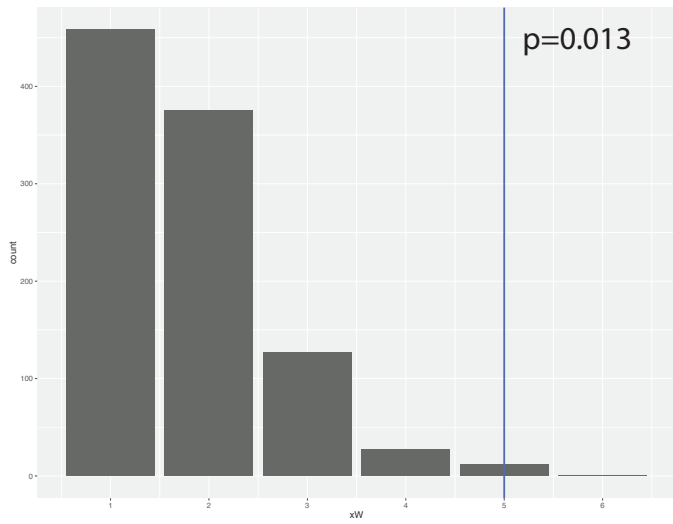
a. HOXA2 targets in permuted selection of 52 genes



HOXA2 targets in permuted selection of 44 genes



b. HOXA2 related genes in permuted selection of 52 genes



HOXA2 related genes in permuted selection of 44 genes

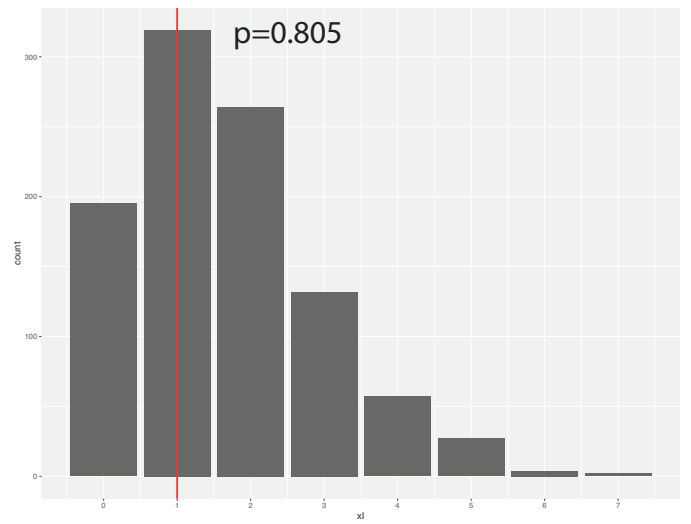


**Figure S10-** Permutation tests for enrichment of *Hoxa2* targets (a) in WT (left, number of *Hoxa2* targets shown as blue dotted line) and inversion (INV) (right, number of *Hoxa2* targets shown as red dotted line). Permutations tests for enrichment of *Hoxa2*-related genes (b) in WT (left, number of *Hoxa2*-related genes shown as blue solid line) and INV (right, number of *Hoxa2*-related genes shown as red solid line).



**Figure S11-** Relative expression of genes in and adjacent to the HOXA cluster at baseline (d0) (a) and after complete CNCC differentiation (d5) (b).

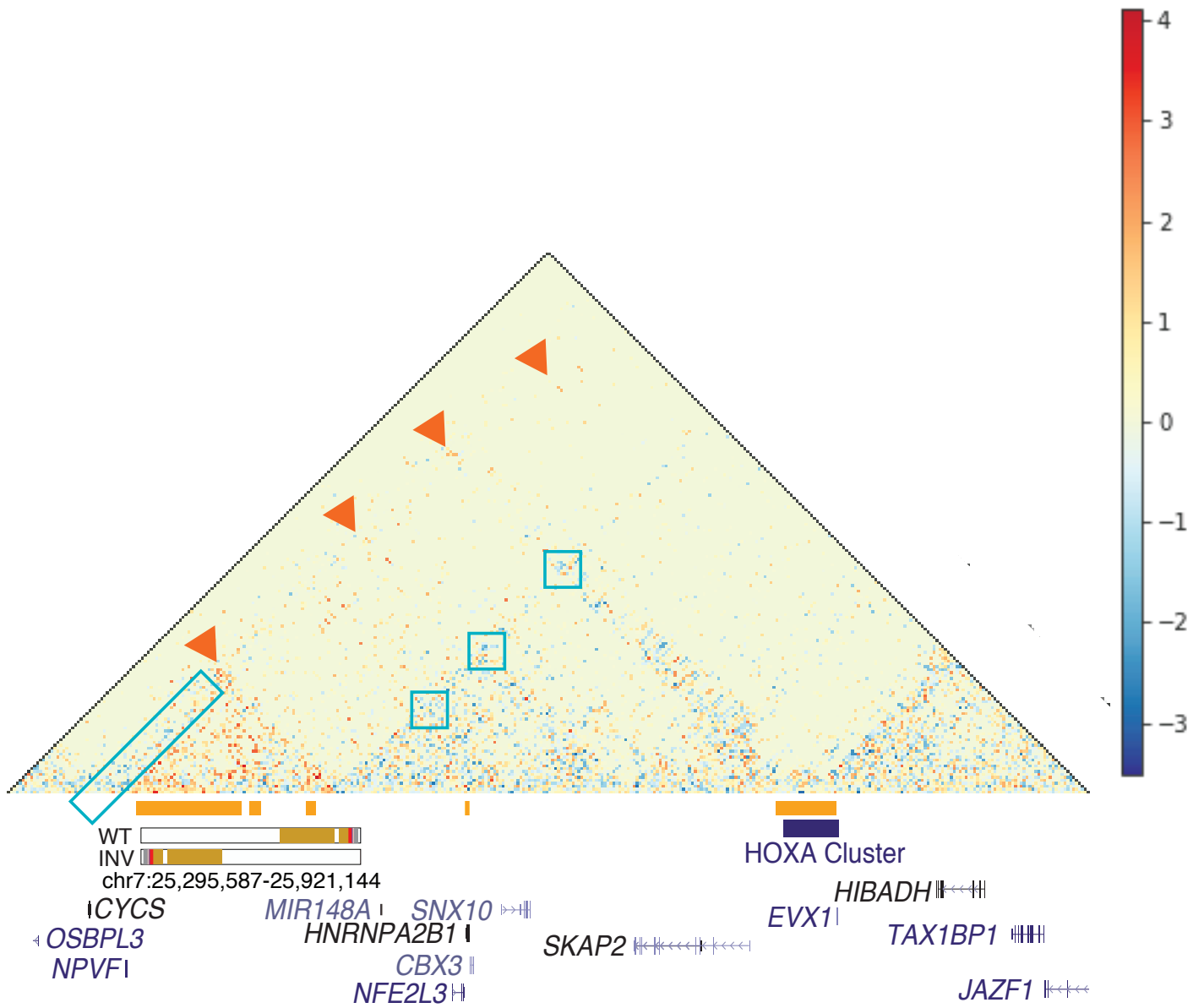


**Figure S12-** Subtraction HiC map generated by comparison of WT CNCC HiC data and INV CNCC HiC data on custom genome accounting for inversion. Representations of the WT and inverted superenhancer region are displayed below the triangular heatmap. Light blue boxes show areas of stronger interaction in the WT CNCCs, red triangles show novel interactions created by the superenhancer inversion.

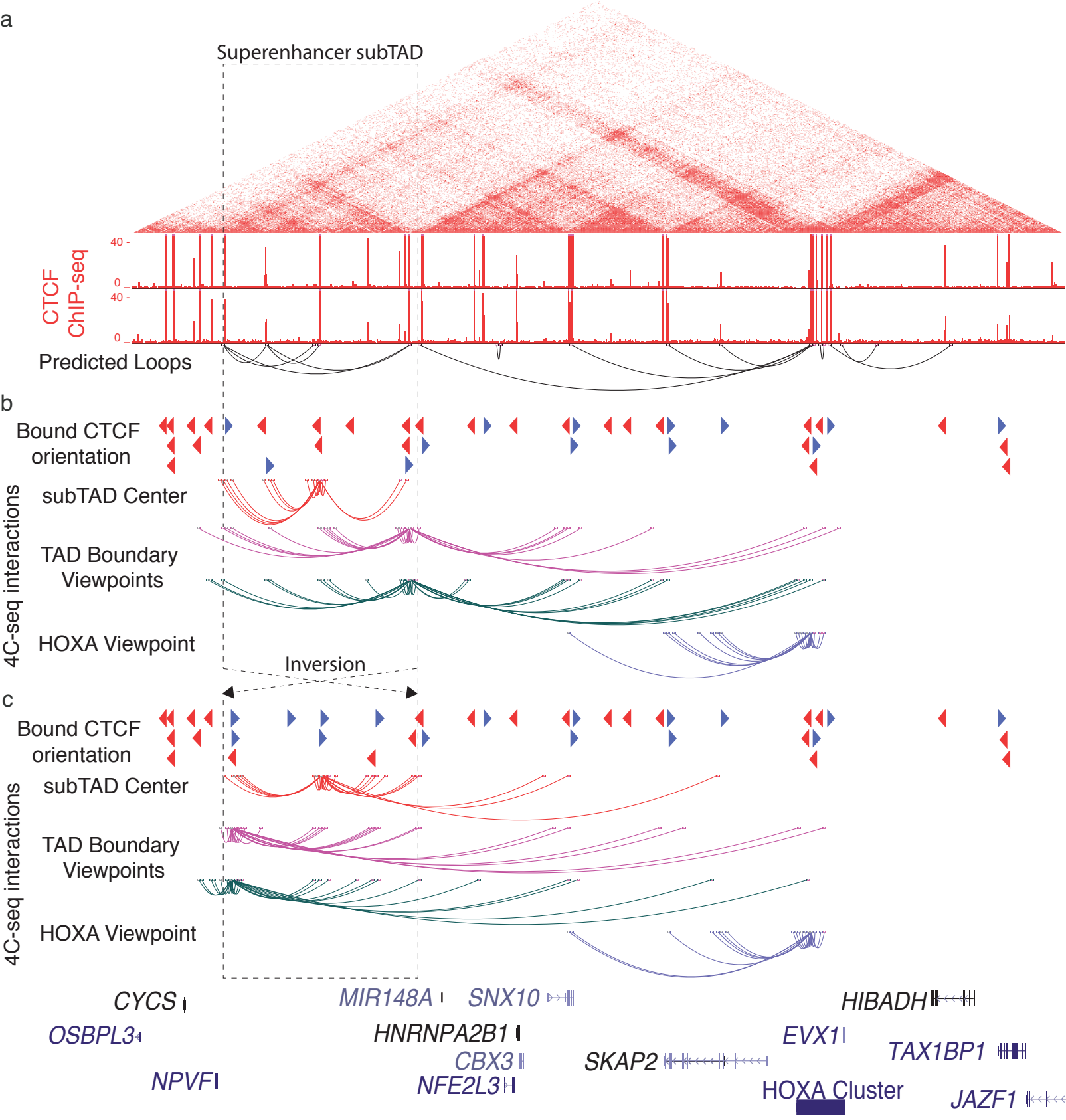
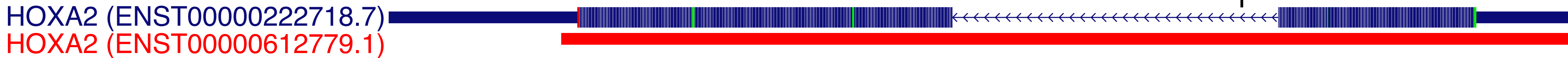




**Figure S13-** Schematic showing consequences of superenhancer inversion on orientation of CTCF sites and boundary strength. Previously insulated 4C viewpoints are capable of interaction with *HOXA* cluster following creation of inversion and viewpoints at the TAD boundary capable of interacting with the *HOXA* cluster in the WT configuration retain contacts following inversion.

a.



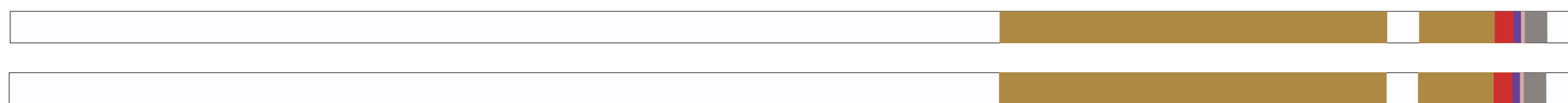
b.

### rs2428431 C/G (%) [counts]

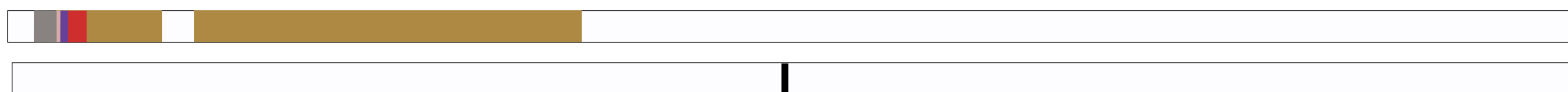
WT n=3: (50%/50%) [3/3]  
 (50%/50%) [5/5]  
 (45%/55%) [5/6]

INV n=3: (17%/83%) [2/10]  
 (33%/67%) [2/4]  
 (21%/79%) [4/15]

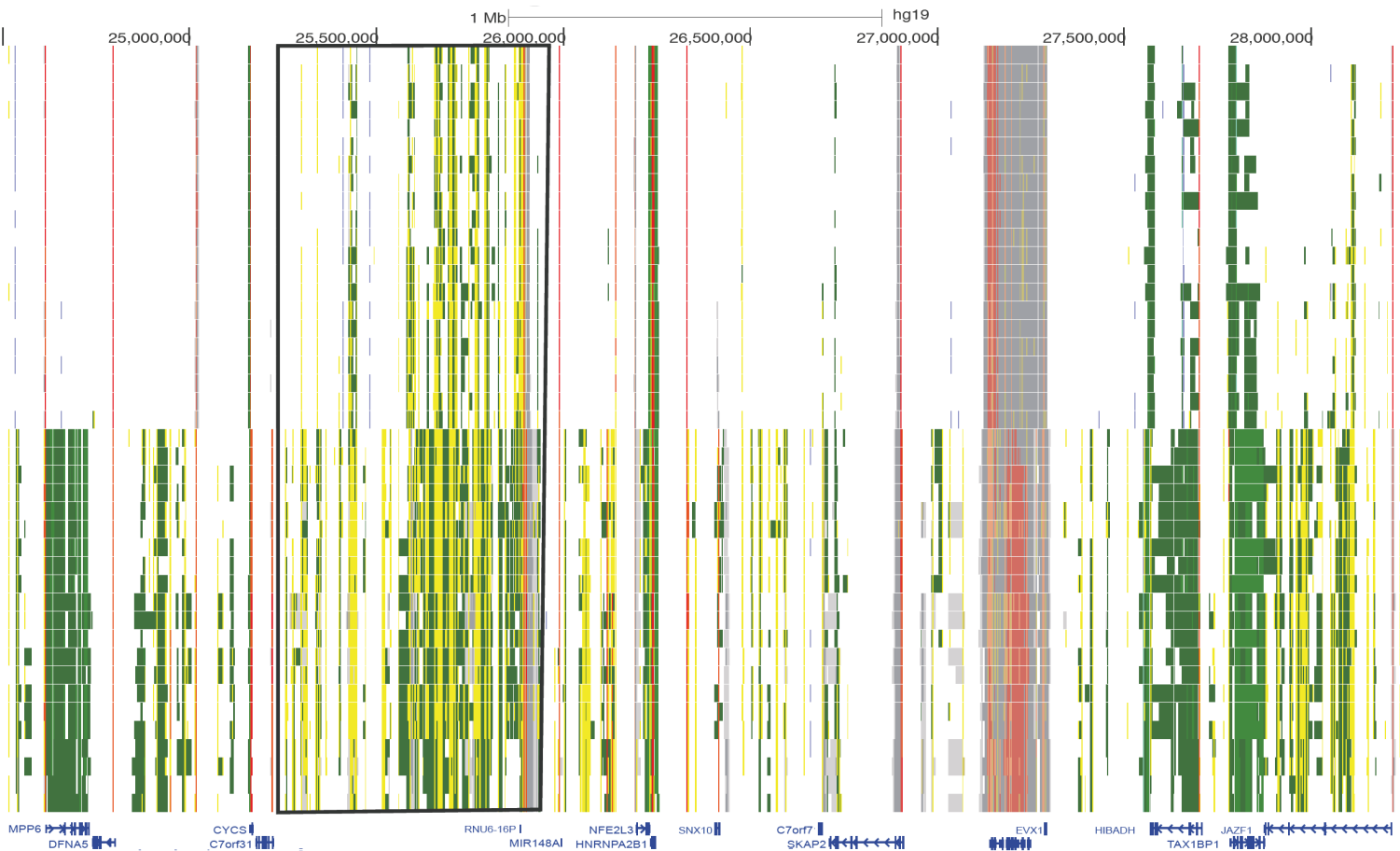
### WT GCR alleles



### Hemizygous inversion of GCR (INV)

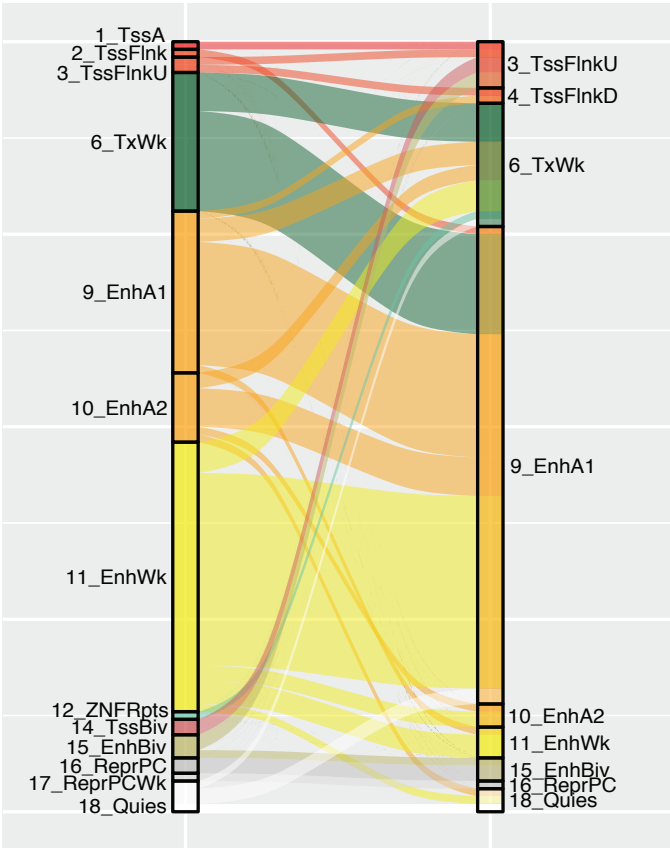


**Figure S14-** IGV browser shot showing C/G allele ratios in WT CNCCs, hemizygous inversion (INV) CNCCs and WT, INV and Heterozygous superenhancer deletion lines in which the TAD boundary of both alleles (WT) or the remaining allele was also deleted.

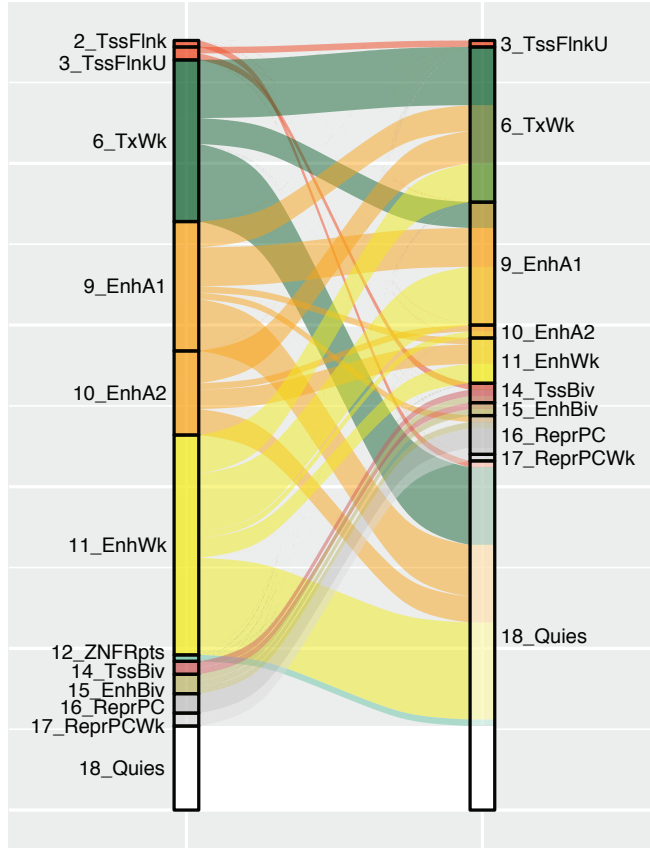
**A**Scale  
chr7:Human Craniofacial  
Chromatin State  
Segmentation  
CS13-CS20, F2  
(15-state model)Mouse Craniofacial  
Chromatin State  
Segmentation  
E9.5-E15.5  
(15-state model)**HOXA Cluster**

**Figure S15-** Comparison of chromatin states in the 15-state model between human embryonic craniofacial tissue (hg19) and mouse embryonic craniofacial tissue (mm9 lifted to hg19).

CS13 craniofacial tissue and E11.5 craniofacial tissue



CS13 craniofacial tissue and E11.5 hindbrain



CS13\_12383

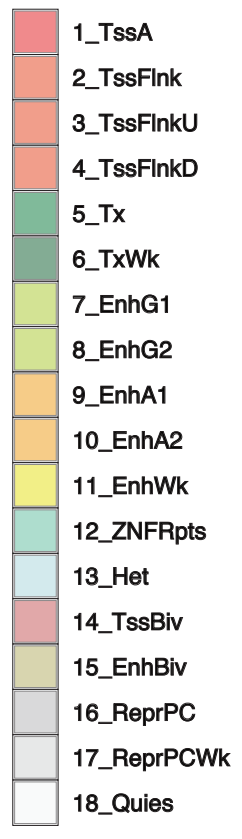


**Figure S16-** Chromatin state composition comparison for 18-state model between CS13 craniofacial tissue and E11.5 craniofacial tissue or E11.5 hindbrain. Mouse chromatin states lifted from mm10 to hg19 using liftOver.

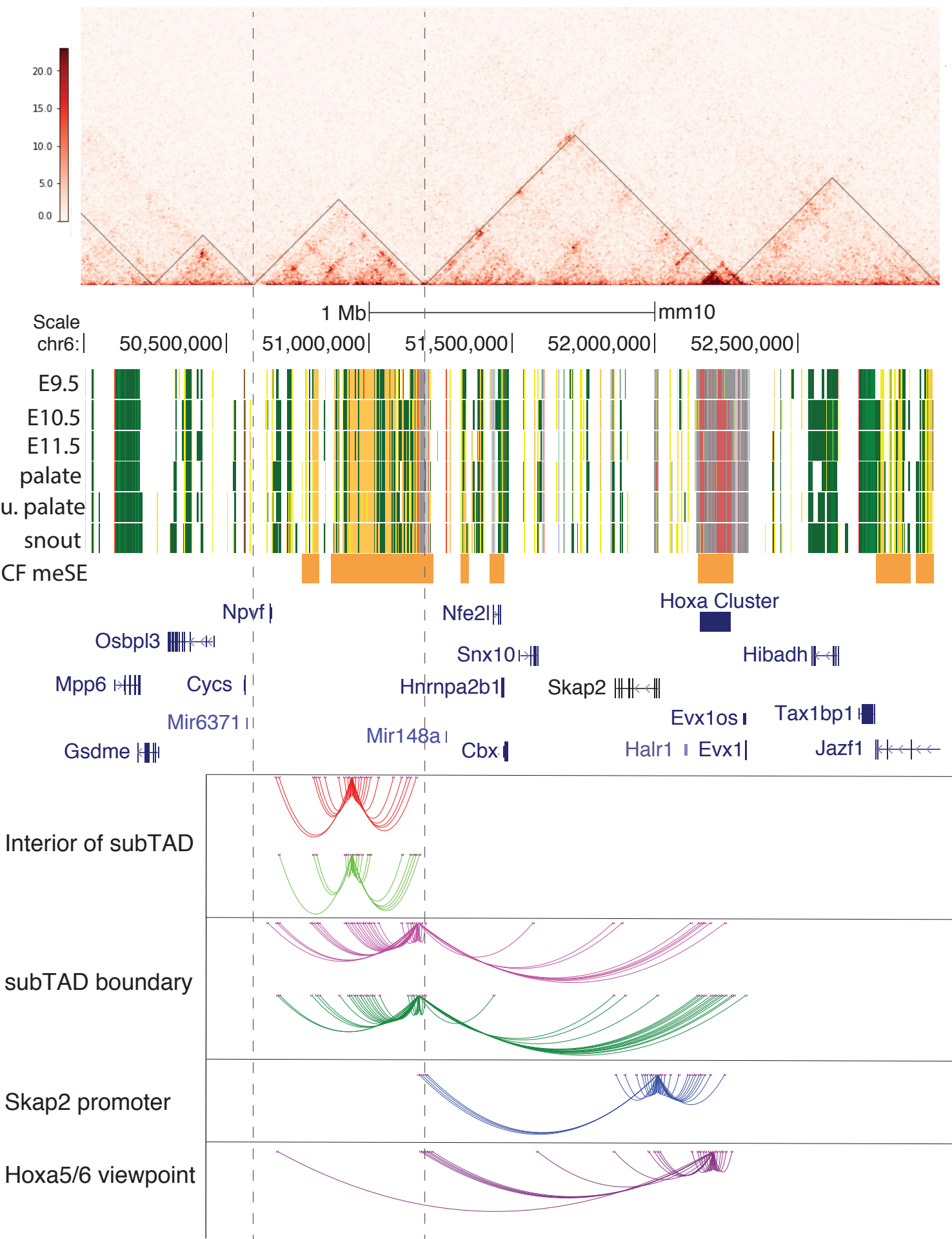




**Figure S17-** HiC data from WT E11.5 mouse craniofacial tissue, TADs or subTADs determined at 50Kb resolution. The superenhancer subTAD is marked throughout with dotted lines (Top). Chromatin states in 18-state model and mouse embryonic craniofacial superenhancers shown in orange bars above gene notations (Middle). Interactions identified through 4C-seq at all viewpoints tested (Bottom). Viewpoint1 (red) and Viewpoint 2 (light green) are located within the interior of the superenhancer subTAD. Viewpoint 3 (magenta) and Viewpoint 4 (dark green) are located at the boundary of the subTAD. Viewpoint 5 (dark blue) is located near the *Skap2* promoter and Viewpoint 6 (purple) is located near the intergenic space between *Hoxa5* and *Hoxa6*.



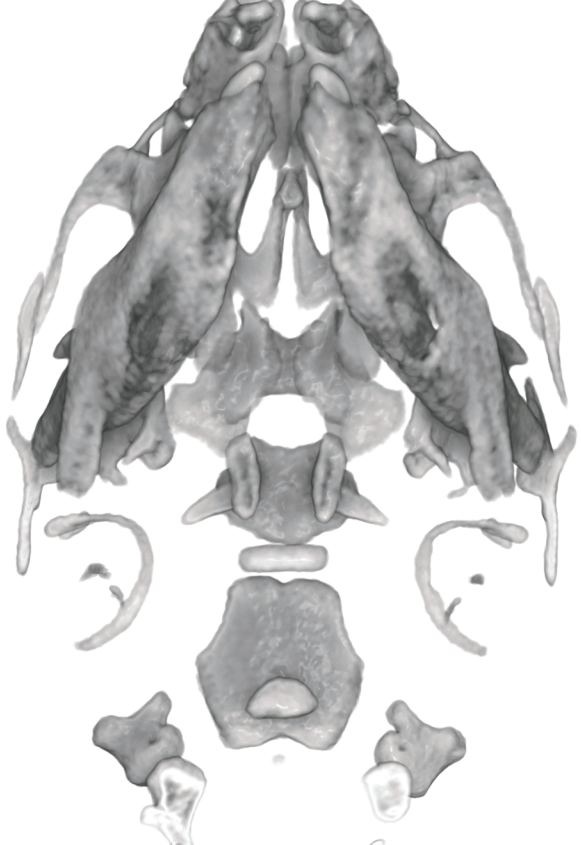
2WT\_Hoxa2 enh\_E18.5\_0S\_CB-ventral.png



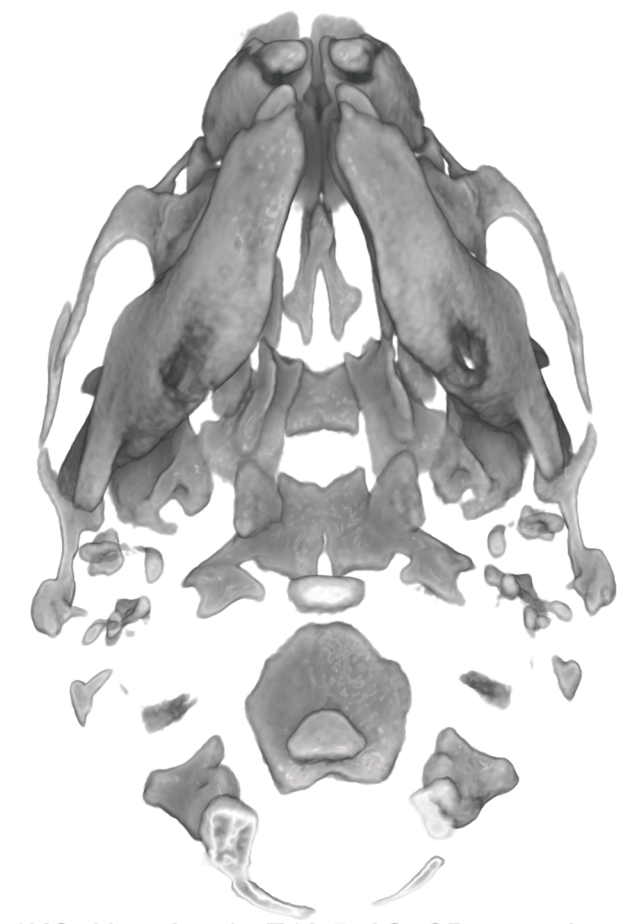
4HT\_Hoxa2 enh\_E18.5\_0S\_CB-ventral.png



11WT\_Hoxa2 enh\_E18.5\_0S\_CB-ventral.png



15HT\_Hoxa2 enh\_E18.5\_0S\_CB-ventral.png



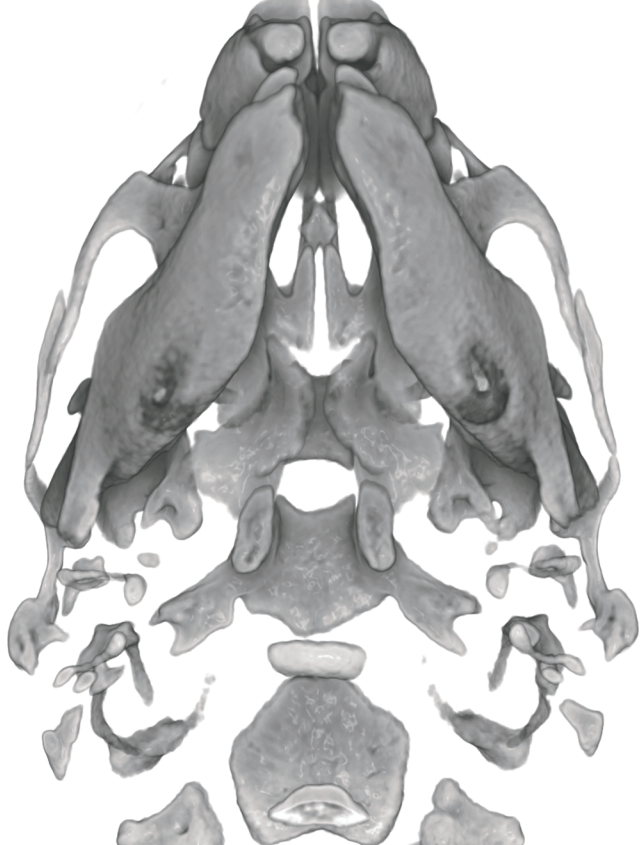
1KO\_Hoxa2 enh\_E18.5\_0S\_CB-ventral.png



3KO\_Hoxa2 enh\_E18.5\_0S\_CB-ventral.png



7KO\_Hoxa2 enh\_E18.5\_0S\_CB-ventral.png



8KO\_Hoxa2 enh\_E18.5\_0S\_CB-ventral.png



9KO\_Hoxa2 enh\_E18.5\_0S\_CB-ventral.png



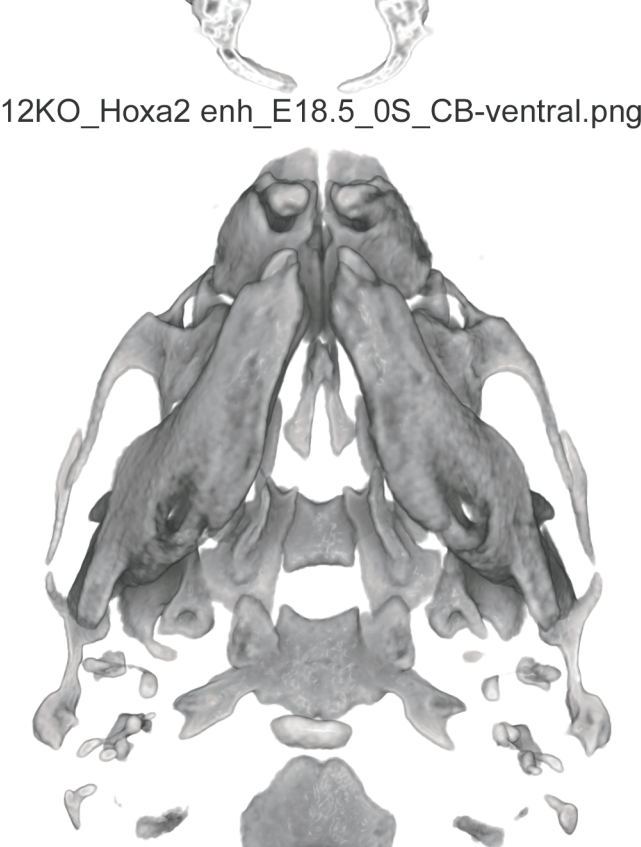
10KO\_Hoxa2 enh\_E18.5\_0S\_CB-ventral.png



12KO\_Hoxa2 enh\_E18.5\_0S\_CB-ventral.png



13KO\_Hoxa2 enh\_E18.5\_0S\_CB-ventral.png



14KO\_Hoxa2 enh\_E18.5\_0S\_CB-ventral.png

**Figure S18-** microCT renderings of skulls from all WT, Hoxa+/ $\Delta$ GCR (HT), and Hoxa  $\Delta$ GCR / $\Delta$ GCR (KO) E18.5 embryos.

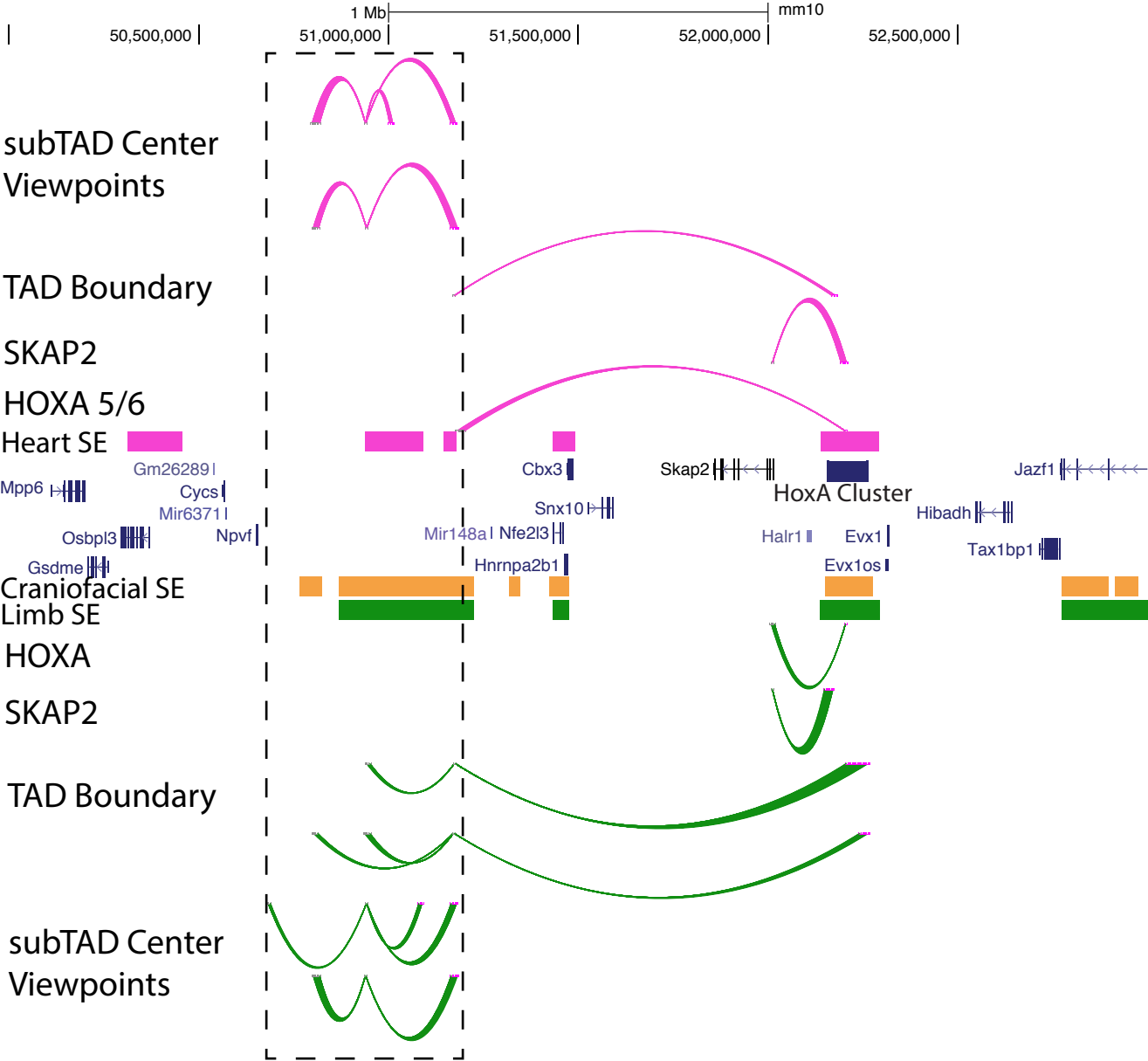


Figure S19 4C-Seq data from E11.5 mouse heart and limb. The superenhancer subTAD is marked throughout with dotted lines. Same viewpoints depicted in Figure S17 were used for each tissue. Interactions identified through 4C-seq are indicated by loops for each viewpoint in heart (pink) and limb (green). Colored bars indicate superenhancer calls in respective tissues.

Craniofacial



PBX1 (p=1e-4)  
Six4 (p=1e-4)  
Pitx1 (p=1e-2)  
GRE (p=1e-2)  
OCT (p=1e-2)

Heart



Mef2d (p=1e-2)

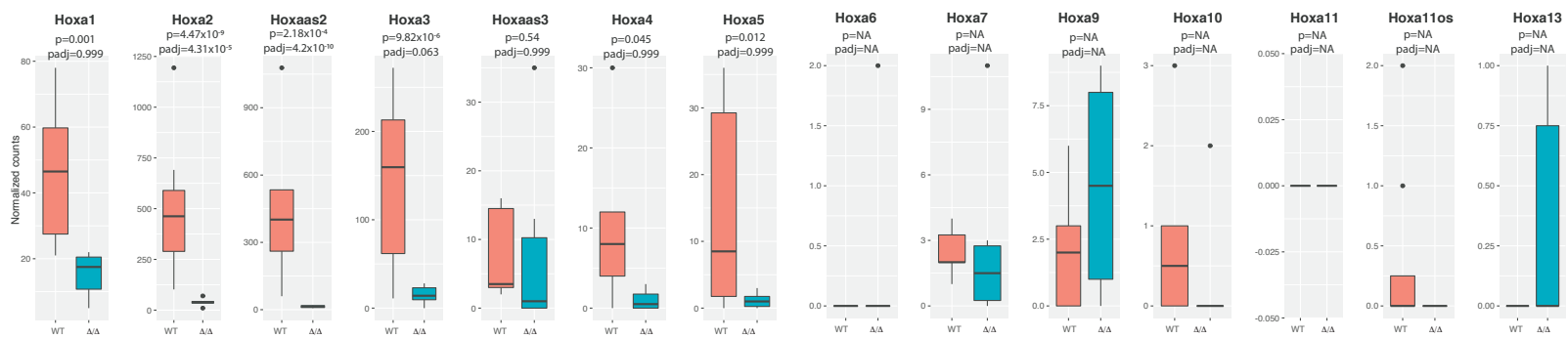
Limb



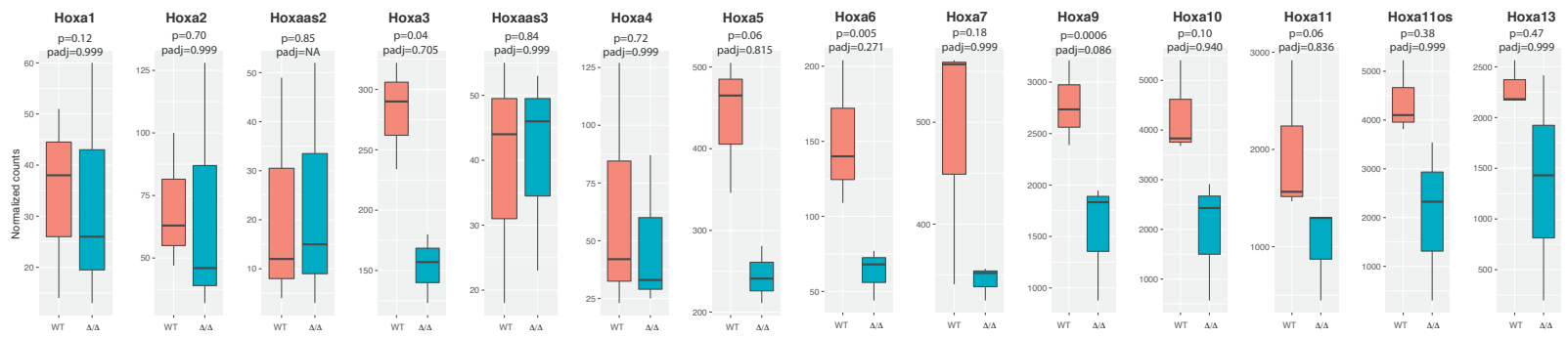
ZNF415 (p=1e-4)  
DMRT6 (p=1e-3)  
GRE (p=1e-3)  
Foxh1 (p=1e-3)  
PBX1 (p=1e-3)  
DMRT1 (p=1e-2)  
ZNF519 (p=1e-2)  
GATA3 (p=1e-2)  
Hoxc9 (p=1e-2)  
MyoD (p=1e-2)  
Pitx1 (p=1e-2)

Figure S20. Significantly enriched TF binding motifs in enhancer modules encompassed by superenhancer calls in the chromosome 7 gene desert.

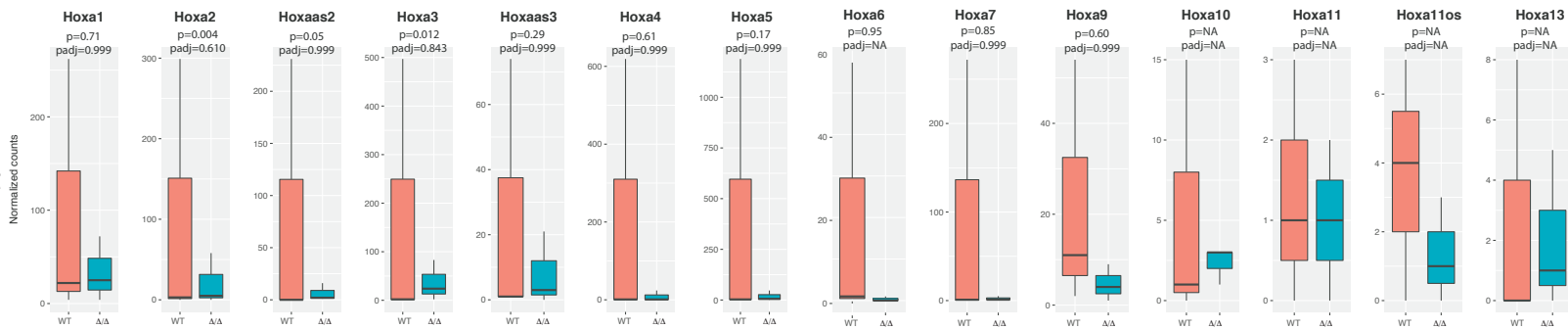
E11.5  
Face



E11.5  
Limb



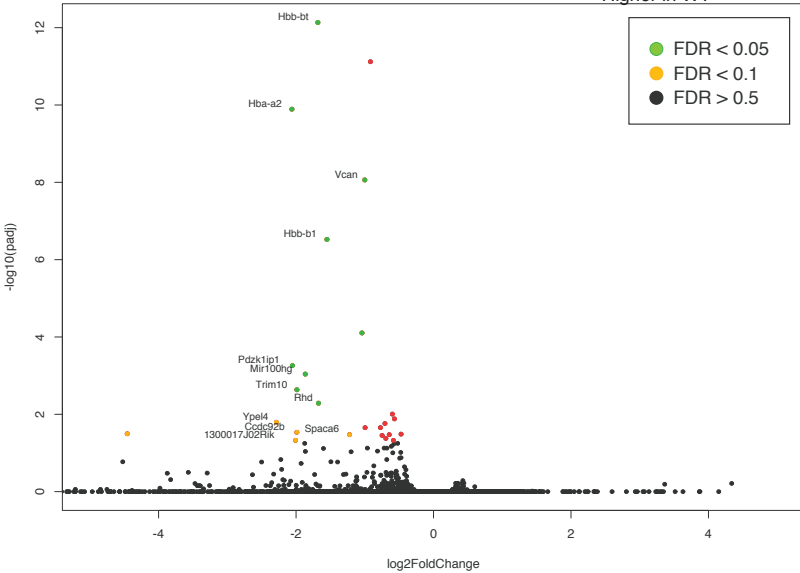
E11.5  
Heart



b

DE Genes  $\Delta GCR/\Delta GCR$  vs WT

Higher in WT



DE Genes  $\Delta GCR/\Delta GCR$  vs WT

Higher in WT

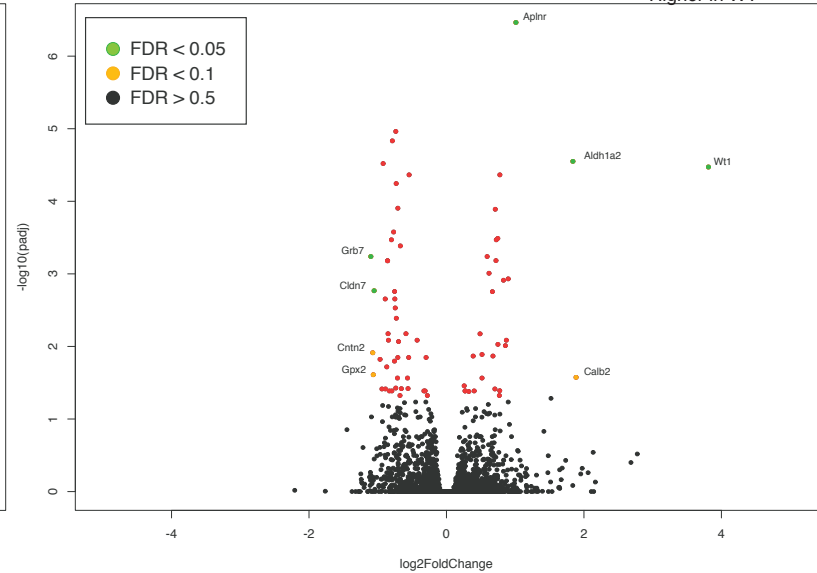




**Figure S21-** Comparison of *Hoxa* gene expression in embryonic face, limb and heart (a). Gene expression changes in heart (b-left panel) and limb (b-right panel). Few significant genes change as a result of the deletion, and did not include the *Hoxa* genes in either heart or limb.

right forelimb: soft tissue morphology

right forelimb: skeletal morphology

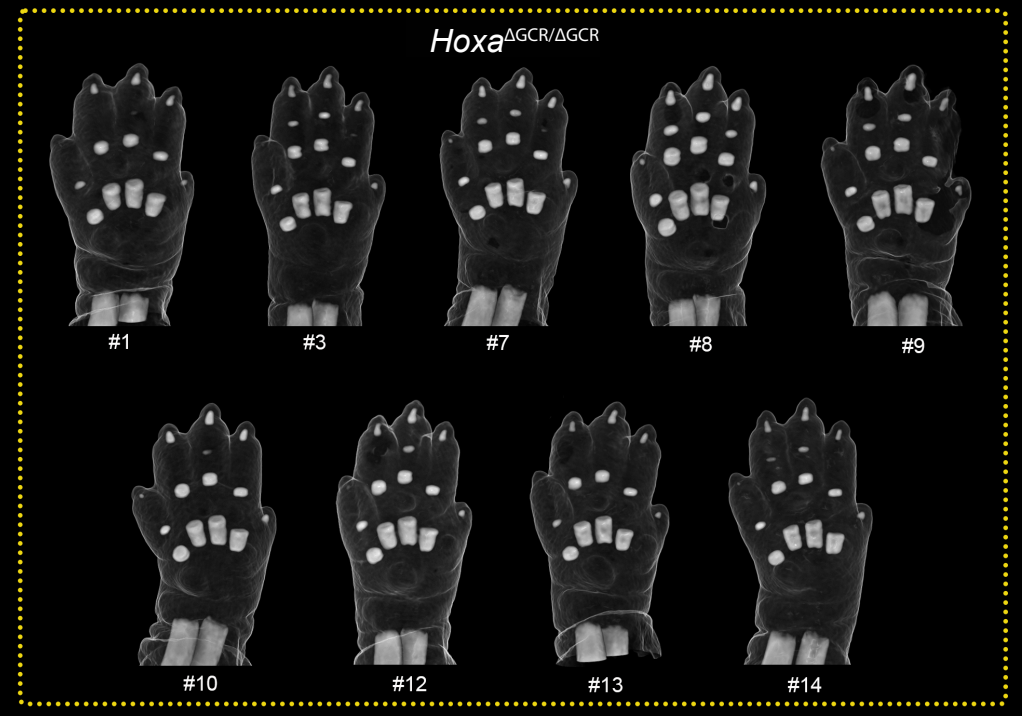


Figure S22. Soft tissue and microCT renderings of limbs from all WT, *Hoxa*<sup>+/ $\Delta$ GCR</sup>, and *Hoxa* <sup>$\Delta$ GCR /  $\Delta$ GCR</sup> E18.5 embryos. Genotypes are indicated in each dashed box and embryos are matched by number across rendering types.



**Figure S23-** a. Deletion of GCR re-structures the *HoxA* regulatory landscape. The removal of ~625kb and almost complete removal of the superenhancers in the gene desert between *Npyf* and *Mir148a* disrupts the contact between the GCR and the *HoxA* cluster. Schematics based on HiC of E11.5 cranofacial tissue from WT (top panel) and  $\Delta$  GCR/  $\Delta$  GCR mice (bottom panel). The bottom panel was created by alignment to a custom genome based on mm10 with deletion of the GCR coordinates. Presentation of superenhancers in the bottom panel are predicted, based on the superenhancers as they appear in the WT. TADs predicted at 100Kb are represented with black outline, TADs predicted at 50Kb have no outline.

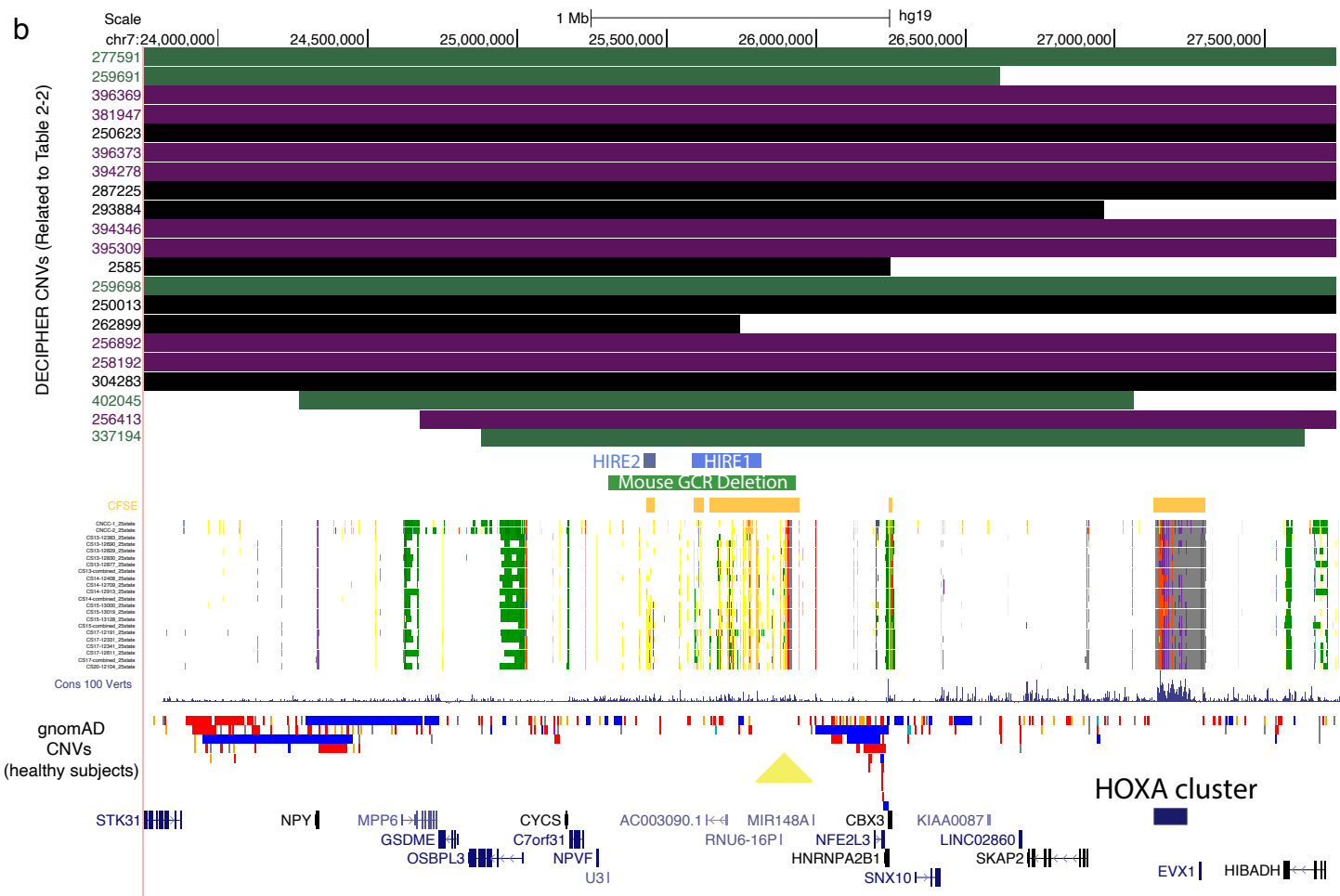
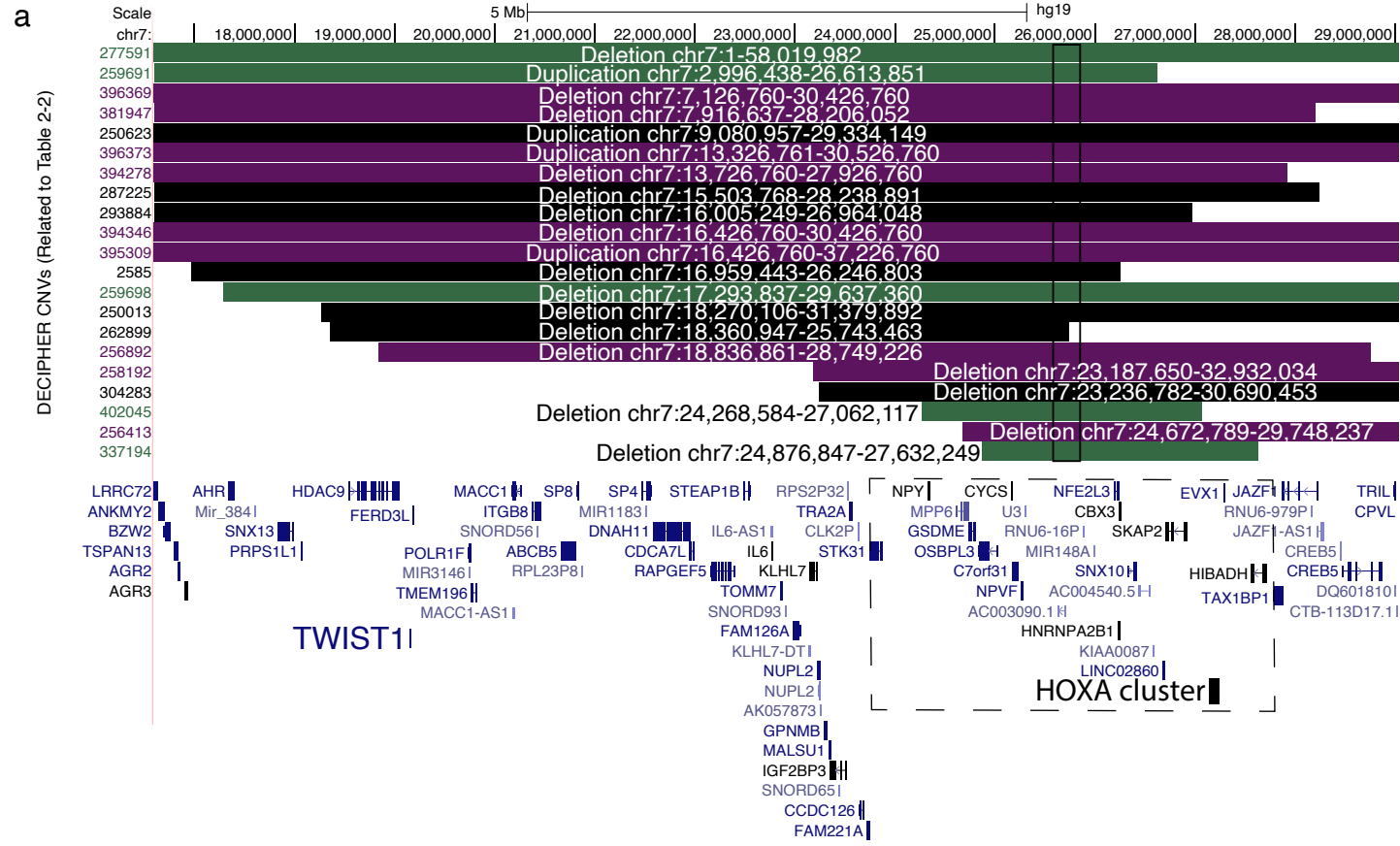


Figure S24. a. Copy number variants from DECIPHER database overlapping the putative novel craniofacial superenhancer region (black box with solid outline). CNVs represented by green bars have a noted phenotype but do not include a specifically described craniofacial phenotype, purple bars have a specifically described craniofacial phenotype and black bars have no phenotype reported. b. Enlargement of region in box with dotted outline. The orthologous positions removed in the GCR deletion mouse are indicated by a green bar. The orthologous positions to HIRE1 and HIRE2 deleted by Kessler et al are shown in shades of blue. Craniofacial superenhancers identified in this study are indicated by large orange bars. The track for gnomAD CNVs, filtered for CNVs >300bp appears below the DECIPHER CNV bars, blue represents gains and red losses. 300bp based on typical size range of CNVs identified in healthy human populations (Zarrei et al., 2015). A region with a notable lack of CNVs in gnomAD subjects is marked by a yellow triangle.

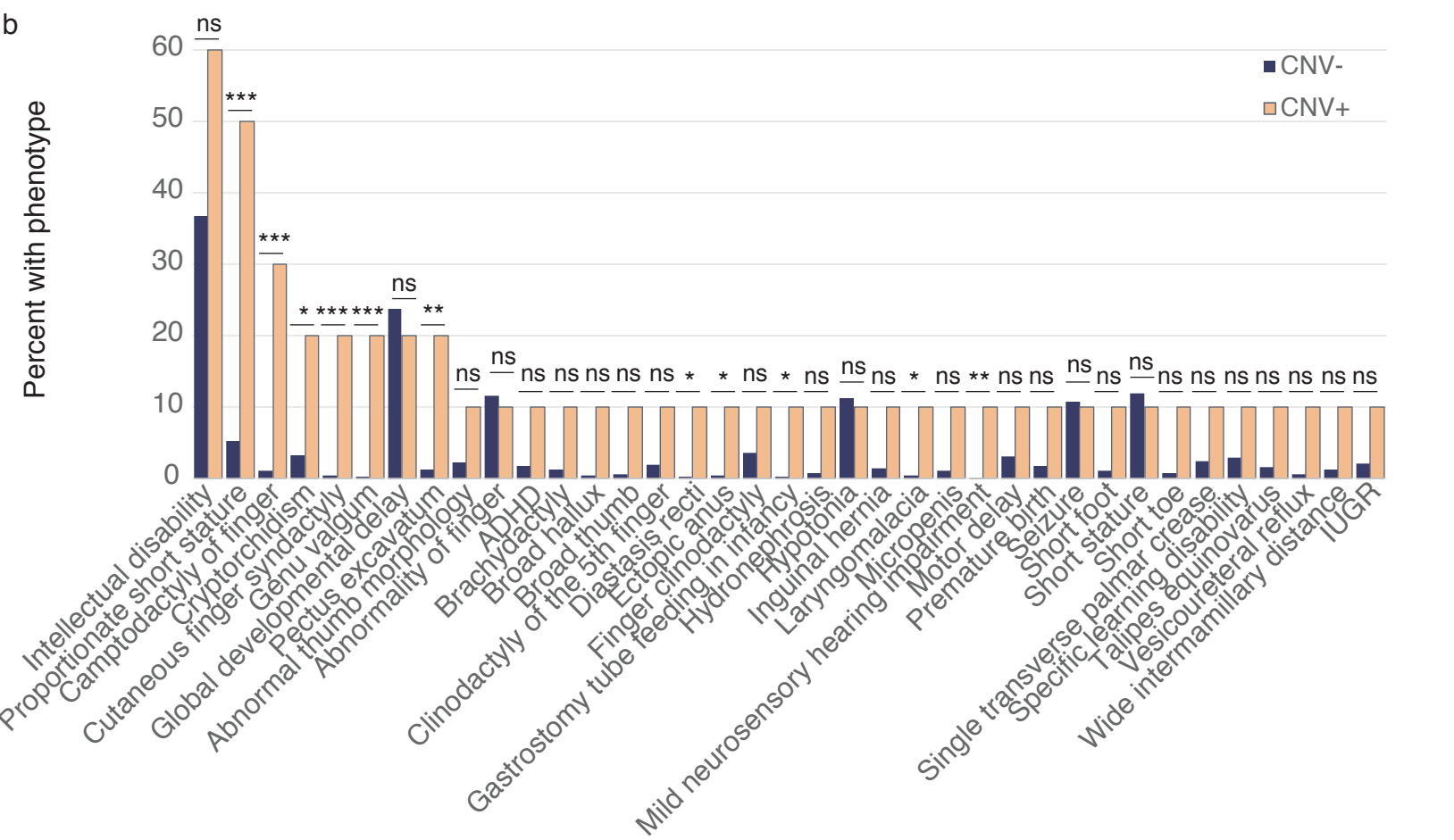
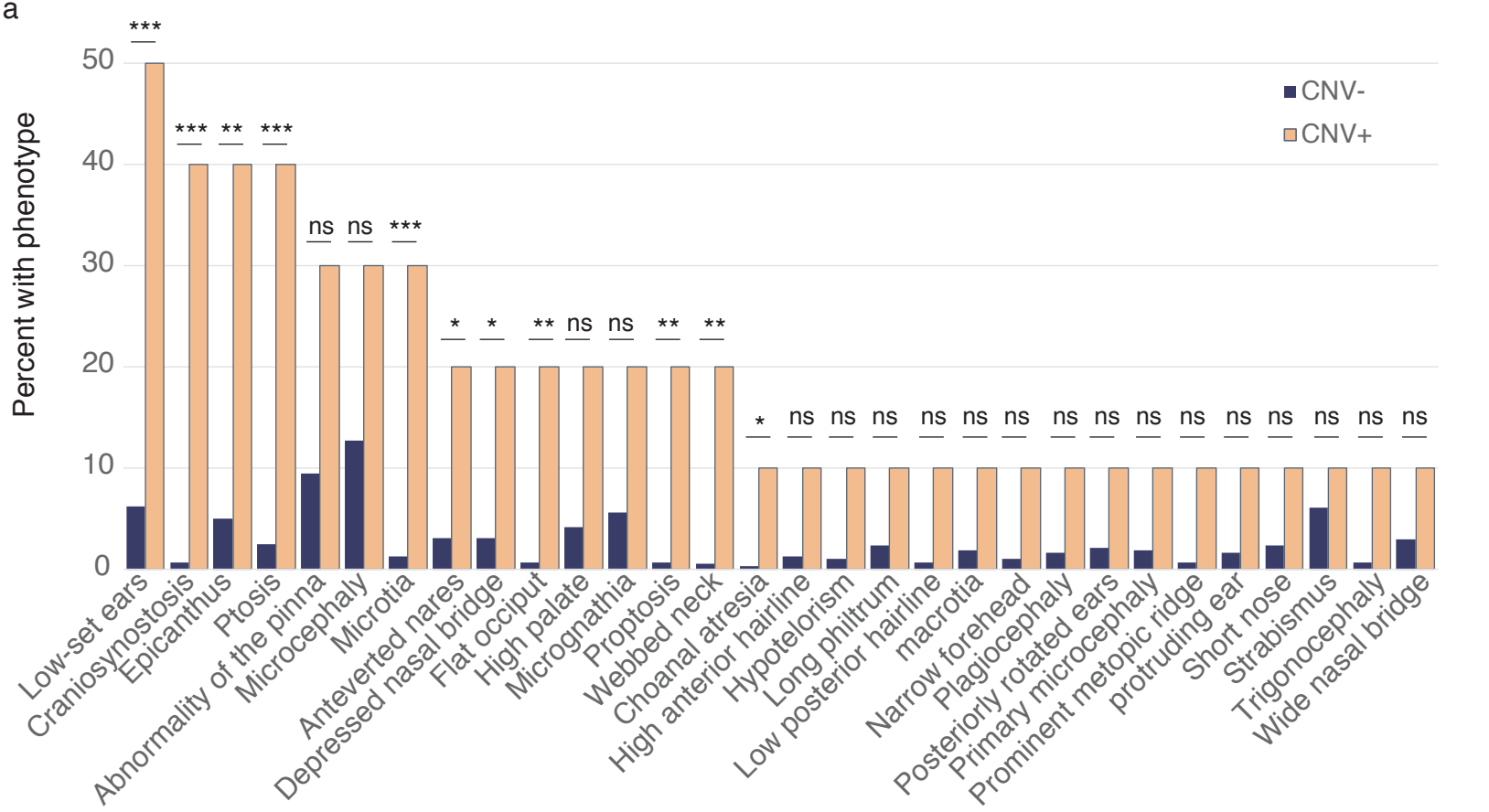
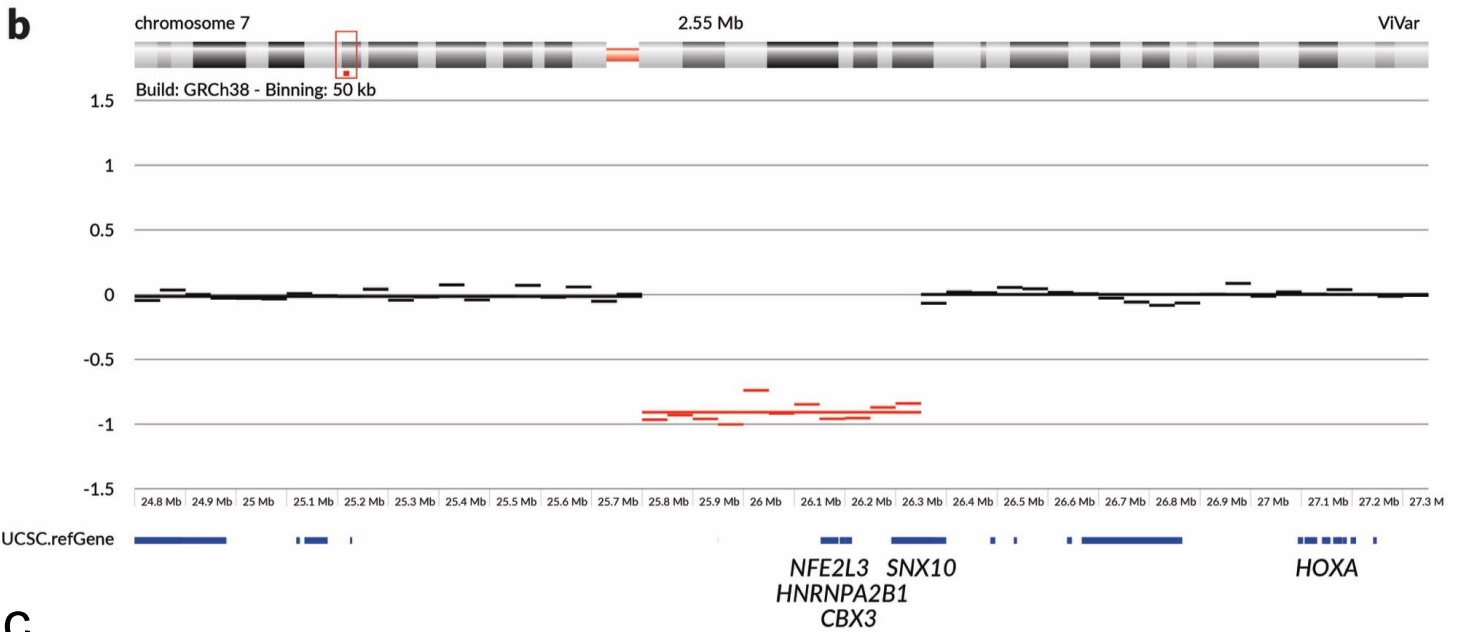
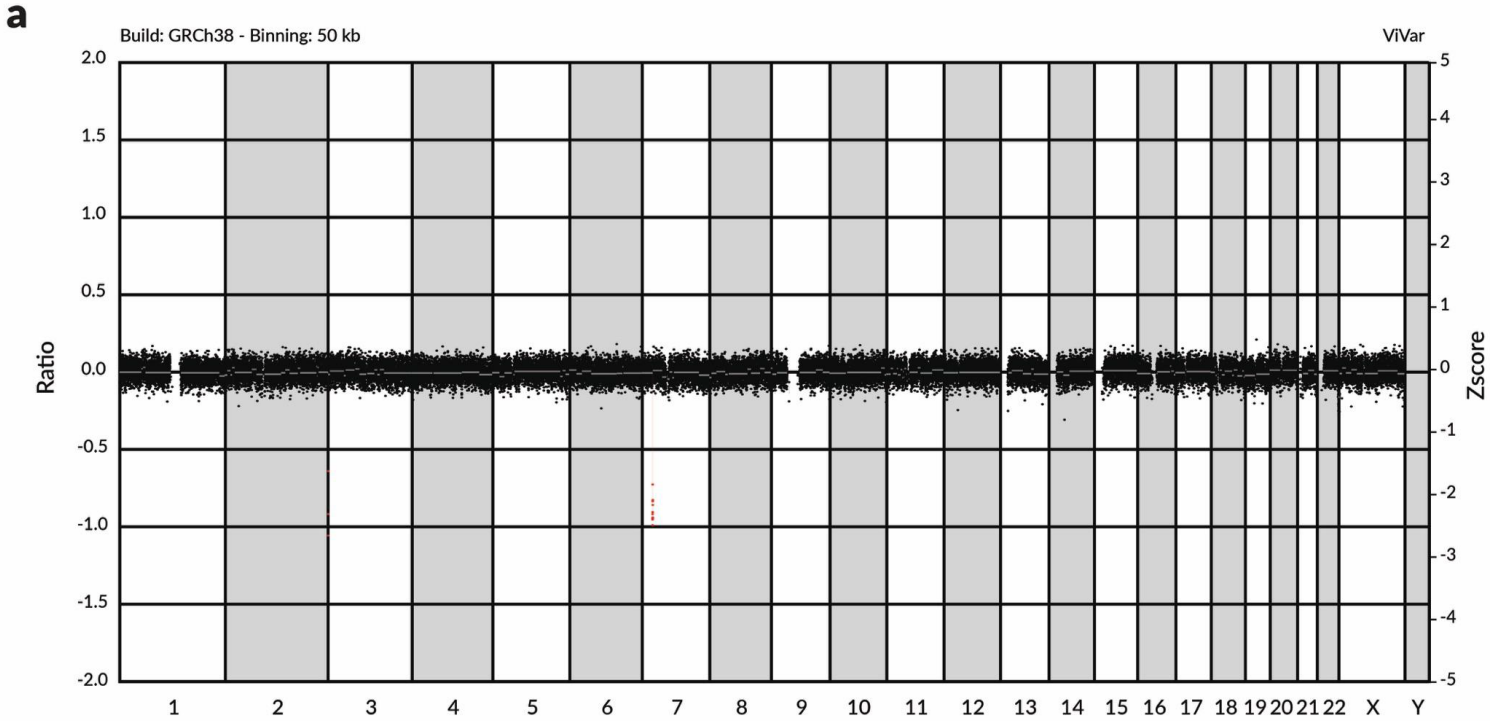




Figure S25. Frequency of phenotypes present in individuals within the DECIPHER Database with CNVs overlapping chr7: 25,580,400-25,849,400 compared to frequency of those phenotypes in the the DECIPHER Database for CNVs not overlapping the region. Statistical test is Fisher Exact Test. \*  $p < 0.05$ , \*\*  $p < 0.01$ , \*\*\*  $p < 0.001$



**Figure S26. Autopsy images of fetus with partial deletion of the HOXA superenhancer region.** The fetus displayed bilateral cleft lip and palate, an underdeveloped nose and only one nostril, clubfeet and anal atresia.



**Figure S27- Identification of a 550kb *de novo* deletion upstream of the *HOXA* cluster through shallow whole genome sequencing and copy-number variant (CNV) analysis using ViVar.** (a) whole genome lineview. (b) zoomed in on deletion (binning: 50kb). ViVar analysis and visualization (Sante et al., 2014). (c). Genome browser view of same region as in (b). At top the *de novo* deletion is indicated in black. The orthologous positions removed in the GCR deletion mouse are indicated by a green bar. The orthologous positions to HIRE1 and HIRE2 deleted by Kessler et al are shown in shades of blue.

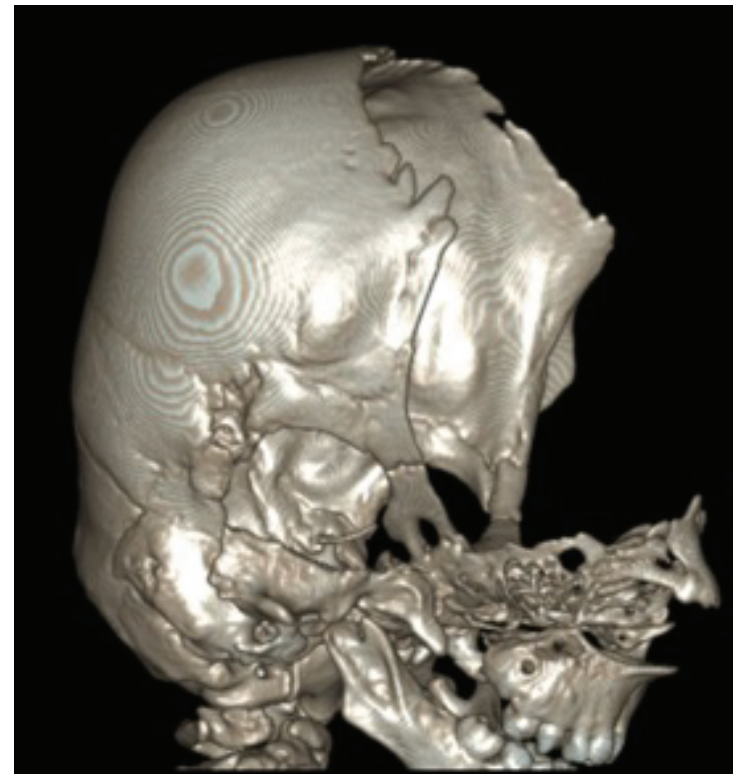
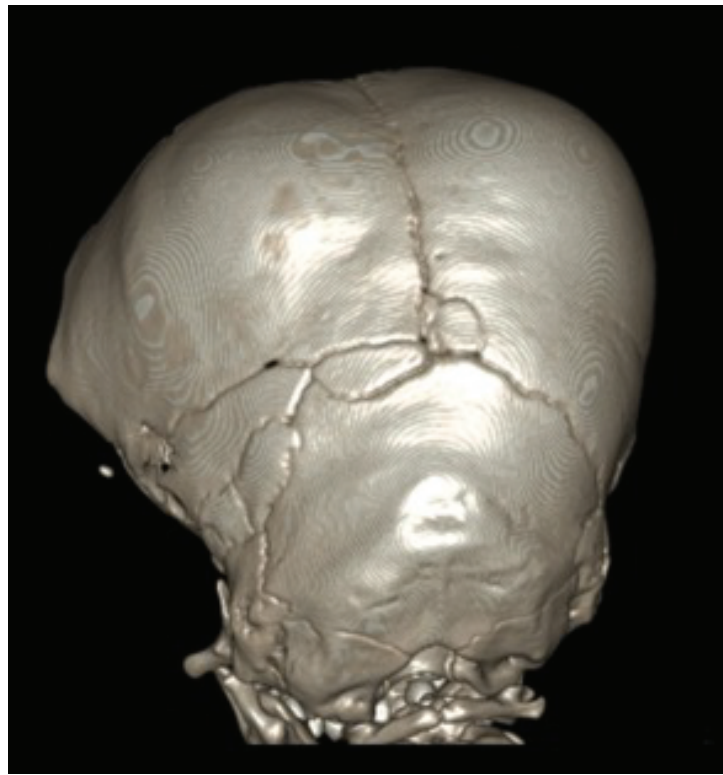
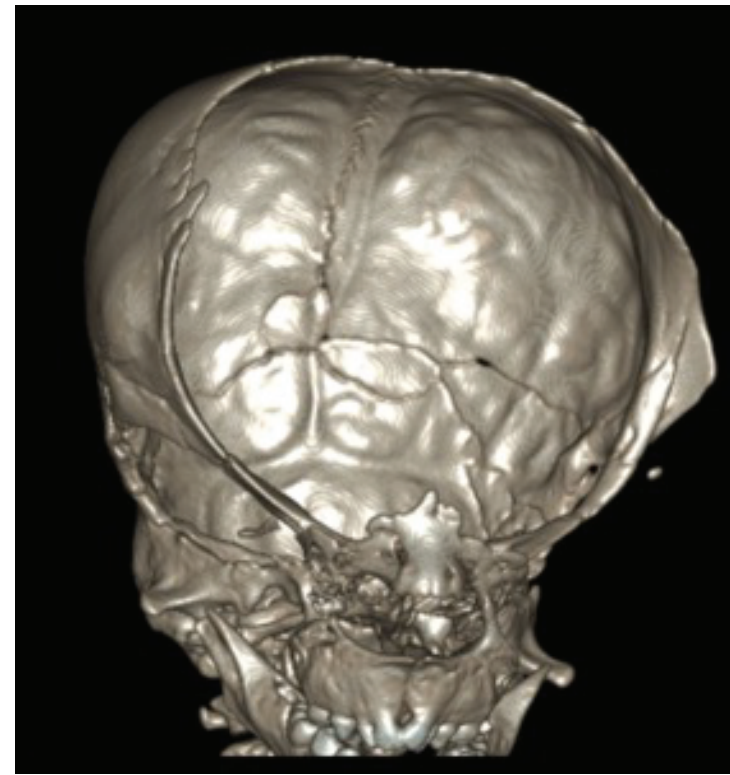
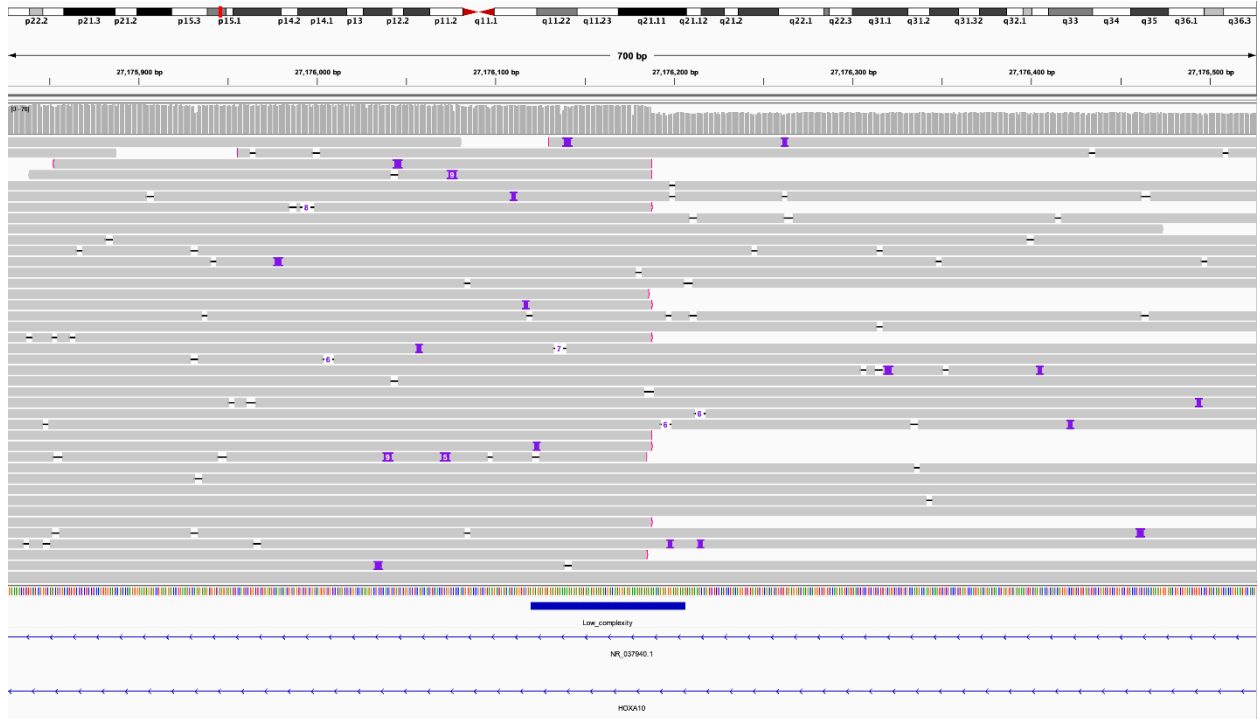


Figure S28. CT scan of patient with in Figure 9 at 18 months of age.



**Fig S29:** Targeted long-read sequencing identified the exact breakpoints of the duplication identified by clinical testing. In the IGV view shown depth of coverage (top track) shows a drop in coverage after the end of the duplication. Orientation of the mapped reads confirm that the duplication is tandem and that the breakpoint at chr7:27,176,187 lies within HOXA10 and a low-complexity GA-rich region. The breakpoint at chr7:25,220,918 is not shown.

## **Supplemental References**

Sante, T., Vergult, S., Volders, P.-J., Kloosterman, W.P., Trooskens, G., De Preter, K., Dheedene, A., Speleman, F., De Meyer, T., and Menten, B. (2014). ViVar: a comprehensive platform for the analysis and visualization of structural genomic variation. *PLoS One* 9, e113800.